

1 Running head: LISSAMPHIBIAN ORIGIN AND OSSIFICATION SEQUENCES

2 Title:

3 What do ossification sequences tell us about the origin of extant amphibians?

4

5 Michel Laurin^{1,*}, Océane Lapauze¹, David Marjanović²

6 ¹ *CR2P (Centre de Recherche sur la Paléodiversité et les Paléoenvironnements; UMR 7207),*

7 *CNRS/MNHN/UPMC–Sorbonne Universités, Muséum national d’Histoire naturelle,*

8 *Département Histoire de la Terre, 57 rue Cuvier, F-75231 Paris cedex 05, France;* ² *Museum*

9 *für Naturkunde (Leibniz Institute for Evolutionary and Biodiversity Research),*

10 *Invalidenstraße 43, D-10115 Berlin, Germany, david.marjanovic@gmx.at*

11 **Correspondence to be sent to: Muséum national d’Histoire naturelle, Département Histoire*

12 *de la Terre, 57 rue Cuvier, F-75231 Paris cedex 05, France; michel.laurin@mnhn.fr*

13

14 ABSTRACT—The controversial origin of extant amphibians has been studied using several
15 sources of data and methods, including phylogenetic analyses of morphological data,
16 molecular dating, stratigraphic data, and integration of ossification sequence data, but a
17 consensus has failed to emerge. We have compiled five datasets to assess the relative support
18 for six competing hypotheses about the origin of extant amphibians: a monophyletic origin
19 among temnospondyls, a monophyletic origin among lepospondyls, a diphyletic origin among
20 both temnospondyls and lepospondyls, a diphyletic origin among temnospondyls alone, and
21 two variants of a triphyletic origin, in which anurans and urodeles come from different
22 temnospondyl taxa while caecilians come from lepospondyls and are either closer to anurans
23 and urodeles or to amniotes. Our datasets comprise ossification sequences of up to 107
24 terminal taxa and up to eight cranial bones, and up to 65 terminal taxa and up to seven
25 appendicular bones, respectively. Among extinct taxa, only two or three temnospondyl can be
26 analyzed simultaneously for cranial data, but this is not an insuperable problem because each
27 of the six tested hypotheses implies a different position of temnospondyls and caecilians
28 relative to other sampled taxa. For appendicular data, more extinct taxa can be analyzed,
29 including some lepospondyls and the finned tetrapodomorph *Eusthenopteron*, in addition to
30 temnospondyls. The data are analyzed through maximum likelihood, and the AICc (corrected
31 Akaike Information Criterion) weights of the six hypotheses allow us to assess their relative
32 support. By an unexpectedly large margin, our analyses of the cranial data support a
33 monophyletic origin among lepospondyls; a monophyletic origin among temnospondyls, the
34 current near-consensus, is a distant second. All other hypotheses are exceedingly unlikely
35 according to our data. Surprisingly, analysis of the appendicular data supports triphyly of
36 extant amphibians within a clade that unites lepospondyls and temnospondyls, contrary to all
37 molecular and recent paleontological phylogenies, but this conclusion is not very robust.

38 **Keywords:** macroevolution; paleontology; evo-devo; ossification sequences; Lissamphibia;

39 Tetrapoda; phylogeny

40

41 **Introduction**

42 Paleontologists have been studying the origin of the extant amphibian clades for more than a
43 century. Early studies generally proposed an origin of at least some extant amphibians from
44 temnospondyls. Cope (1888) initially suggested that batrachians (anurans and urodeles)
45 derived from temnospondyls (a large clade of limbed vertebrates known from the Early
46 Carboniferous to the Early Cretaceous) because he believed that the batrachian vertebral
47 centrum was an intercentrum, the dominant central element of temnospondyls. Later, Watson
48 (1940) argued that anurans were derived from temnospondyls because of similarities (mostly
49 in the palate) between the temnospondyl “*Miobatrachus*” (now considered a junior synonym
50 of *Amphibamus*) and anurans. Monophyly of extant amphibians (Lissamphibia) was proposed
51 by Parsons and Williams (1962, 1963), an idea that was accepted more quickly by
52 herpetologists than by paleontologists. Lissamphibian monophyly was supported by (among a
53 few other character states) the widespread occurrence of pedicellate, bicuspid teeth. The
54 subsequent discovery of such teeth in the amphibamid temnospondyl *Doleserpeton* (Bolt
55 1969) reinforced the widespread acceptance of an origin of Lissamphibia from within
56 temnospondyls (e.g., Schoch and Milner 2004). Recently, this hypothesis, referred to as the
57 temnospondyl hypothesis or TH for short (Fig. 1c), has been supported by several
58 phylogenetic analyses based on phenotypic data matrices (e.g. Ruta and Coates 2007;
59 Sigurdsen and Green 2011; Maddin et al. 2012; Pardo et al. 2017a, b: fig. S6; Mann et al.
60 2019).

61 Dissenting opinions about the origin of extant amphibians have been expressed for
62 several decades (see Schoch and Milner 2004 for a historical review). These were initially
63 formulated especially for the urodeles and caecilians, which are less similar to temnospondyls
64 and lack a tympanic middle ear (which is present in most anurans and often inferred for at
65 least some temnospondyls but absent in lepospondyls). Thus, Steen (1938) highlighted

66 similarities in the palate (broad cultriform process of the parasphenoid) and cheek (loss of
67 several bones) between lysorophian lepospondyls and urodeles. Carroll and Currie (1975) and
68 Carroll and Holmes (1980) argued that the extant amphibians had three distinct origins among
69 early stegocephalians; while they accepted an origin of anurans among temnospondyls, they
70 suggested that urodeles and caecilians originated from two distinct groups of lepospondyls
71 (*Rhynchonkos* for caecilians, Hapsidopareiidae for urodeles). Later, based mostly on
72 developmental similarities between the temnospondyl *Apateon* and urodeles, Carroll (2001,
73 2007) and Fröbisch et al. (2007) proposed another hypothesis involving a triphyletic origin of
74 lissamphibians, with an origin of anurans and urodeles from two distinct temnospondyl
75 groups, while the caecilians would remain in the lepospondyl clade. This is what we call the
76 polyphyly hypothesis (PH). We have tested two versions. One (called PH1; Fig. 1e) was
77 cautiously suggested by Fröbisch et al. (2007); it agrees with the paleontological consensus in
78 placing all or most lepospondyls closer to Amniota than to Temnospondyli (Fig. 1b;
79 Sigurdson and Green 2011; Pardo et al. 2017a, b: fig. S6; Marjanović and Laurin 2019; Clack
80 et al. 2019; Mann et al. 2019). The other (PH2; Fig. 1f) is modified to make Lissamphibia
81 monophyletic with respect to Amniota, a fact we consider demonstrated beyond reasonable
82 doubt by multiple phylogenetic analyses of molecular data (Fig. 1a; Irisarri et al. 2017; Feng
83 et al. 2017; and references cited therein); this comes at the expense of contradicting the
84 paleontological consensus, which was not yet established when Milner (1993: 16–18, fig. 5B)
85 argued for something like the PH2 as one of two more or less equal possibilities. Anderson
86 (2007) and Anderson et al. (2008) found lissamphibian diphyly, specifically a monophyletic,
87 exclusive Batrachia among the temnospondyls while keeping the caecilians among the
88 lepospondyls (DH1; Fig. 1g). Pardo et al. (2017b: fig. 2, S7) presented a similar hypothesis,
89 with batrachians and caecilians having separate origins within the temnospondyls (DH2; Fig.
90 1h). Further, a monophyletic origin of all extant amphibians among lepospondyls has also

91 been proposed (Laurin 1998; Pawley 2006: appendix 16; Marjanović and Laurin 2009, 2013,
92 2019). This will be referred to below as the lepospondyl hypothesis (LH; Fig. 1d).

93 Phylogenetic analyses of molecular data cannot distinguish the TH, the PH2, the DH2
94 or the LH from each other by topology (Fig. 1) because all of these imply lissamphibian
95 monophyly with respect to amniotes. Several other types of data and methods have, however,
96 been used to try to discriminate between the various hypotheses on the origin of extant
97 amphibians. In addition to classical phylogenetic analyses of morphological data matrices,
98 these include the use of molecular dating (Zhang et al. 2005; Marjanović and Laurin 2007;
99 Pardo et al. 2017b) and stratigraphic data (Marjanović and Laurin 2008) to compare the
100 inferred divergence dates between the three main extant amphibian clades on the basis of
101 molecular data with predictions based on the fossil record under the TH and the LH on the
102 one side and the PH and the DH on the other. However, developmental data, in the form of
103 ossification sequences, have been the second-most frequently used (after classical
104 morphological data) to argue for particular phylogenetic hypotheses. These data include
105 mainly cranial (e.g. Schoch 2002, 2006; Schoch and Carroll 2003; Schoch and Milner 2004;
106 Anderson 2007; Carroll 2007; Germain and Laurin 2009) and autopodial ossification
107 sequences (e.g. Fröbisch et al. 2007, 2015). Ossification sequences of other parts of the
108 skeleton, like the vertebrae, shoulder girdle and scales, are also documented in a few
109 Paleozoic stegocephalians (e.g. Carroll et al. 1999; Witzmann and Schoch 2006; Anderson
110 2007; Carroll 2007; Olori 2013), not to mention finned tetrapodomorphs (Cloutier 2009), but
111 these have played a minor role in the controversy about the origin of extant amphibians, and
112 recently, Danto et al. (2019) concluded that vertebral ossification sequences varied too
113 quickly and could not be used to assess the origin of lissamphibians. This study relies on both
114 cranial and appendicular ossification sequences and compares their implications for tetrapod
115 phylogeny.

116 METHODS

117 *Ossification sequence data*

118 From all the literature we could access, we compiled the most extensive database on
119 ossification sequences for osteichthyans that exists to date. The most useful sources for extant
120 taxa included compilations: Harrington et al. (2013) for amphibians, Weisbecker and
121 Mitgutsch (2010) for anurans, Hugi et al. (2012) for squamates, Maxwell et al. (2010) for
122 birds, and Koyabu et al. (2014) and Weisbecker (2011) for mammals. The cranial and
123 appendicular sequences of Permian temnospondyls (the stereospondylomorphs
124 *Sclerocephalus* and *Archegosaurus*, the non-branchiosaurid “branchiosaur” *Micromelerpeton*
125 and the branchiosaurids “*Melanerpeton humbergense*, *Apateon caducus* and *A. pedestris*)
126 were assembled from several references cited in the Appendix; note that the two *Apateon*
127 species are each represented by two different sequences scored after populations from two
128 separate paleo-lakes (Erdesbach and Obermoschel) in which both species occur. Appendicular
129 ossification sequences of the lepospondyls *Microbrachis* and *Hyloplezion* are incorporated
130 from Olori (2013), that for the finned tetrapodomorph *Eusthenopteron* was combined from
131 Cote et al. (2002) and Leblanc and Cloutier (2005).

132 All sources of our sequence data can be found in the Appendix. The sequences
133 themselves and the phylogenetic trees corresponding to the tested hypotheses are included in
134 the supplementary material. The sequences were not used to generate the tree topology or the
135 branch lengths (which represent evolutionary time); the tree is compiled from published
136 sources (provided below) which did not use any ossification sequences in their phylogenetic
137 analyses.

138 The software we used to compute AICc weights, the CoMET module (Lee et al. 2006)
139 for Mesquite 3.6 (Maddison and Maddison 2018), cannot handle missing data. This

140 unfortunately meant we had to discard much information. In order to keep as many taxa as
141 possible in the analysis, we first compiled a matrix (not shown) of 244 taxa and 213
142 characters. All of these characters are positions of skeletal elements (cranial, appendicular,
143 axial and others) in ossification sequences, standardized between 0 and 1 following Germain
144 and Laurin (2009), as explained below. Of these, we kept characters that were scored in the
145 Paleozoic taxa in our initial database, and extant taxa that were scored for the same sets of
146 characters. This resulted in two initial datasets, one of cranial and one of appendicular
147 sequences (it was not possible to include both sets of sequences together because this would
148 have left too few taxa in the matrix). In the end, we were left with three overlapping cranial
149 datasets. Dataset 1 contains 107 taxa (104 extant, *Apateon* spp. from Erdesbach, and
150 *Sclerocephalus*) and only six characters. Dataset 2 (see Table 1) has 105 taxa (103 extant, plus
151 the two species of *Apateon* scored from Erdesbach) and seven characters (nasal, parietal,
152 squamosal, premaxilla, maxilla, pterygoid, and exoccipital); The third cranial dataset (dataset
153 5) includes 84 taxa (81 extant, *Apateon* spp. from Erdesbach, and *Sclerocephalus*) and eight
154 cranial characters (the frontal bone is added). For the appendicular characters, in addition to
155 dataset 3 which contains seven characters (humerus, radius, ulna, ilium, femur, tibia and
156 fibula) and 62 taxa (54 extant, *Apateon* spp. from Obermoschel, *Sclerocephalus*,
157 *Archegosaurus*, *Micromelerpeton*, *Hyloplezion*, *Microbrachis* and *Eusthenopteron*), another
158 (dataset 4) includes only four characters (radius, ulna, ilium, and femur), but it features 65
159 sequences, the additional data being *Apateon* spp. from Erdesbach and “*Melanerpeton*”
160 *humbergense*. See Table 1 for a list of these datasets and the SM for the datasets themselves.

161 The data loss in these various datasets is not as severe as it may first seem, because
162 most of the characters that have collectively been excluded from these analyses had less than
163 10% scored cells (sometimes less than 1%), and most of them could not be scored for any

164 temnospondyl or lepospondyl, so they could not have helped resolve the main question
165 examined in this study.

166 The order in which the eight cranial bones ossify varies substantially in our sample of
167 taxa, but based on simple (not phylogenetically-weighted) average position, the frontal
168 appears first, followed closely by the premaxilla, parietal, and maxilla (in close succession),
169 and then by the squamosal, exoccipital, pterygoid, and last by the nasal. However, all of these
170 bones ossify first (among these seven bones; not necessarily in the whole skeleton) in at least
171 one of the included taxa. Among the appendicular bones, there is more variability; all ossify
172 first in at least one of the 62 sampled taxa, and three (radius, ulna and ilium) ossify last in at
173 least one taxon.

174 Of the eight cranial characters, *Sclerocephalus* cannot presently be scored for the
175 squamosal. Because of the potential importance of *Sclerocephalus* as a stem-caecilian
176 according to the DH2 (Fig. 1h) and as one of only three sampled extinct taxa with any known
177 cranial ossification sequence, we ran variants of the analyses of cranial data with
178 *Sclerocephalus* and six characters (dataset 1), and without *Sclerocephalus* and with seven
179 characters (dataset 2; see Table 1).

180 Due to the homology problems between the skull bones of tetrapods and
181 actinopterygians and missing data, we had to omit all actinopterygians from our analyses. As
182 cranial ossification sequences remain unknown for extant finned sarcopterygians (except
183 perhaps lungfish, whose skull bones seem mostly impossible to homologize), our analyses of
184 those data are restricted to limbed vertebrates. However, for appendicular data, we were able
185 to include the Devonian tristichopterid *Eusthenopteron foordi*.

186 Unfortunately, the only cranial ossification sequence available for any supposed
187 lepospondyl, that of the aïstopod *Phlegethontia longissima*, is documented from only three

188 ossification stages (Anderson et al. 2003; Anderson 2007). This poses a problem for our
189 analysis method, which assumes that character evolution can be modeled as Brownian
190 motion; this assumption is decreasingly realistic as the number of character states (sequence
191 positions) decreases, because the resulting distribution deviates increasingly from that of a
192 continuous character. Furthermore, some recent anatomical restudies and phylogenetic
193 analyses suggest that aïstopods are not lepospondyls, but early-branching stem-
194 stegocephalians (Pardo et al. 2017a, 2018; Mann et al. 2019; Clack et al. 2019).

195 The low taxon sample is more limiting for this analysis than the low character sample.
196 However, as explained below, the absence of lepospondyl sequences in our cranial dataset
197 does not preclude testing the six hypotheses (TH, PH1, PH2, DH1, DH2, LH; see above or
198 Figure 1 for the explanation of these abbreviations) because each of these six hypotheses
199 makes different predictions about where temnospondyls and caecilians fit relative to other
200 taxa. Thus, in the absence of lepospondyls in our dataset, the tests of these hypotheses are
201 somewhat indirect and inference-based, but they remain possible. Our tests based on
202 appendicular data include two lepospondyls (*Hyloplesion longicostatum* and *Microbrachis*
203 *pelikani*), but the absence of caecilians in that dataset proves more limiting than the absence
204 of lepospondyls in the cranial dataset because the TH, DH1 and DH2 become
205 indistinguishable (Fig. 1 c, g, h). However, the presence of lepospondyls allows us to test two
206 variants of the TH/DH distinguished by the monophyly (e.g. Ruta and Coates 2007) or
207 polyphyly (e.g. Schoch 2019) of “branchiosaurs” (the temnospondyls *Apateon*,
208 “*Melanerpeton*” and *Micromelerpeton*).

209 *Sensitivity analysis for sequence polymorphism*

210 Given the potential impact of infraspecific variability in ossification sequence on inferred
211 nodal sequences and heterochrony (Olori 2013; Sheil et al. 2014), we compiled two consensus

212 sequences for *Apateon caducus* and *A. pedestris* each, representing two localities where both
213 species occur, the paleo-lakes of Erdesbach (Schoch 2004) and Obermoschel (Werneburg
214 2018). Based on dataset 4 (see Table 1), we incorporated these into a global and two separate
215 analyses (one analysis per locality) to determine the impact of the observed variability.
216 Incorporating the sequences from Erdesbach reduced the number of characters from seven to
217 only four because the software used cannot handle missing data (see below), but this
218 information loss is compensated by the great increase in number of sequences from extinct
219 taxa (eleven instead of two, when counting the sequences of *Apateon* from both localities
220 separately) and the fact that this includes some lepospondyls (see below). It would have been
221 even better to perform a sensitivity analysis incorporating variability for all taxa for which
222 such information was available, but given the scope and nature of our study, this would have
223 been exceedingly time-consuming and is best left for the future.

224 *Standardization of the data*

225 Given that various taxa differ in their numbers of bones and that the resolution of the
226 sequences is also variable between taxa, these data needed to be standardized to make
227 comparisons and computations meaningful, as suggested by Germain and Laurin (2009).
228 Note that we performed this standardization on the complete dataset of characters, before
229 filtering for data completeness. This complete dataset (not shown) includes 213 cranial,
230 appendicular and other characters, but no taxon is scored for all characters, given that the
231 original (complete) matrix has much missing data. For instance, the most completely scored
232 taxon, *Amia calva*, still has 57.4% missing data (more than half), which indicates that 92
233 characters were scored for this taxon, including several ties (the resolution was 41 positions,
234 so they varied by increments of 0.025 or 2.5% of the recorded ontogeny). We did not re-
235 standardize after filtering characters out because we believe that the initial standardization
236 better reflects the relative position of events in development than a standardization based on

237 only seven events in ontogeny would. Because of this, in the reduced dataset of seven
238 characters used in the calculations, for some taxa, no character has a score of 0 or 1 because
239 the first or last events in the ontogenetic sequence were filtered out. Thus, we used the
240 position in the sequence (from first to last, in the complete dataset) and standardized this
241 relative sequence position between 0 and 1 using the simple formula given by Germain and
242 Laurin (2009). The standardized sequence position (X_s) is:

$$243 \quad X_s = (X_i - X_{\min}) / (X_{\max} - X_{\min}),$$

244 where:

245 X_i is the position of a given bone in the sequence

246 X_{\min} is the lowest position in the sequence (generally denoted 0 or 1)

247 X_{\max} is the highest position in the sequence (for instance, if there are 20 bones, X_{\min} is 1 and
248 the sequence is completely resolved, $X_{\max} = 20$).

249 This yields a standardized scale that varies between 0 and 1 for each taxon, in which 0 and 1
250 are the positions of the first and last events in the sequence, respectively. For instance, for
251 *Ambystoma maculatum* (an extant urodele), in the original dataset, the first events (tied) were
252 the ossification of premaxilla, vomer, dentary and coronoid (standardized position: 0); the last
253 event was the articular (standardized position: 1), and there is a resolution of 12 positions
254 (hence, increments of 0.0909 or 1/11). However, in the final dataset of 7 characters, the
255 articular is absent; hence, the first bone in the sequence is the premaxilla, at a standardized
256 position of 0, and the last is the nasal, as a standardized position of 0.8181 because all events
257 in position 1 (articular) and 0.9091 (stapes) have been filtered out.

258 We also experimented with using size (skull length) or developmental stage as standards, but
259 this led to lower sequence resolution because body size is not available for all sequence

260 positions and for all taxa (results not shown), so we worked only with sequences standardized
261 using sequence position. Given that our data filtering procedure retains little data (only six,
262 seven or eight characters for the cranial dataset, and four or seven characters for the
263 postcranial dataset), it is important to use the method that discards the least amount of data,
264 and this was achieved by using sequence position. We do not imply that standardizing by size
265 is not recommended in general. On the contrary, if good body size data were available for all
266 taxa and all developmental stages, this should be a better strategy, and only having access to
267 absolute time should be even better. However, practical limitations of data availability prevent
268 us from using these methods now.

269 Our ossification sequence data (reduced dataset of four to eight characters) of extant
270 and extinct taxa, and the phylogenetic trees we used, are available in the supplement to this
271 paper.

272 *Analysis methods*

273 To discriminate between the six hypotheses about the origin of extant amphibians, two
274 methods are available: direct phylogenetic analysis of the sequence data, and comparisons of
275 the tree length (number of steps in regular parsimony, squared length in squared-change
276 parsimony, likelihood, or similar measures) of various trees selected a priori to represent these
277 hypotheses (in these trees, only the position of caecilians and extinct taxa, here temnopondyls
278 and lepospondyls, varies). We used both approaches but expected the second to perform much
279 better because relatively few data are available, and thus, phylogenetic analysis of such data is
280 unlikely to provide a well-resolved tree.

281 For the first approach, we first transformed the standardized sequence positions back
282 into discrete characters using formulae in a spreadsheet and scaled the characters so that the
283 highest state in all would be 9. This ensures that each character has an equal weight in the

284 analysis, regardless of its variability in the ossification sequence. The characters were ordered
285 to reflect the assumed evolutionary model (ontogenetic timing is a quantitative character that
286 was discretized) and because for such characters, ordering yields better results (Rineau et al.
287 2015, 2017; see discussion in Marjanović & Laurin 2019). The resulting data matrices (one
288 for cranial and another for appendicular characters, both with seven characters each) were
289 analysed using parsimony in PAUP* 4.0a165 (Swofford 2019). We used the TBR (tree
290 bisection-reconnection) branch swapping algorithm and performed a search with 50 random
291 addition replicates (or several such searches, for the cranial data) while holding two trees at
292 each step and with a maximal number of trees set at one million. For cranial data, the main
293 search lasted about 100 hours on a MacBook Pro Retina with a 2.5 GHz iCore 7 quadri-core
294 processor and 16 GB RAM. The exact search time cannot be reported because PAUP*
295 crashed after saving the trees to a file for one of the longest runs (several analyses were made,
296 over several days), but before the log could be saved. The analysis of the seven appendicular
297 characters was much faster (27 minutes and a half), presumably because that matrix has fewer
298 taxa (62 instead of 105).

299 For the second approach (comparison of fit of various trees selected a priori to reflect
300 previously published hypotheses), we used the CoMET module (Lee et al. 2006) for Mesquite
301 3.6 (Maddison and Maddison 2018) to test the relative fit of the data on trees representing the
302 six hypotheses. CoMET calculates the likelihood and the AIC (Akaike Information Criterion)
303 of nine evolutionary models given continuous data and a tree. Note that our data only
304 represent an approximation of continuous data; if standardization had been performed on
305 developmental time or body size, the data would actually have been continuous.
306 Standardization was carried out using sequence position because of data limitation problems,
307 so the data actually follow a decimalized meristic scale. However, the difference between
308 these situations decreases as the number of sequence positions increases, and our global scale

309 includes up to 41 positions (and an average of 10.9 positions), so our data should approximate
310 a continuous distribution sufficiently well for our analyses to be valid. This consideration
311 prevents us from adding the highly apomorphic aïstopod *Phlegethontia*, for which only three
312 cranial ossification stages are known (Anderson et al. 2003; Anderson 2007); moreover, five
313 of the seven bones included in our analyses appear in the last two of these stages, and two of
314 the relevant bones (parietal and exoccipital) are not present as separate ossifications, which
315 would create additional missing data. In that case, the very low number of stages would create
316 strong departures from the assumption of continuous data. This would probably create
317 statistical artifacts, and the uncertainty about the position of *Phlegethontia* (Pardo et al.
318 2017a, 2018; Marjanović and Laurin 2019; Clack et al. 2019) would complicate interpretation
319 of the results.

320 The nine models evaluated by CoMET are obtained by modifying the branch lengths
321 of the reference tree. Thus, branches can be set to 0 (for internal branches only, to yield a non-
322 phylogenetic model), to 1 (equal or speciation model), left unchanged from their original
323 length (gradual evolution), or set free and evaluated from the data (free model). This can be
324 applied to internal and/or external branches, and various combinations of these yield nine
325 models (Lee et al. 2006: fig. 1). Among these nine models two have been frequently discussed
326 in the literature and are especially relevant: gradual evolution, in which branch lengths (here
327 representing evolutionary time) have not been changed, and a speciation model, in which all
328 branches are set to the same length, and which has some similarities with Eldredge and
329 Gould's (1972) punctuated equilibria model (though a model with one internal branch
330 stemming from each node set to 0 and the other set to 1 would be even closer to the original
331 formulation of that model). In this study, we assessed the fit of six of the nine models covered
332 by CoMET; the other three (the punctuated versions of distance [original branch length],
333 equal and free) in which the one of each pair of daughter-lineages has a branch length of zero,

334 could not be assessed due to problems in the current version of CoMET and possibly the size
335 of our dataset.

336 Provided that the same evolutionary model is optimal for all compared phylogenetic
337 hypotheses (this condition is met, as shown below), the AIC weights of the various trees
338 under that model can be used to assess the support for each tree. In such comparisons, the
339 topology is part of the evolutionary model, and the data are the sequences. These comparisons
340 can show not only which tree is best supported, but how many times more probable the best
341 tree is compared to the alternatives. This quantification is another reason to prefer this
342 approach over a phylogenetic analysis (performed below, but with the poor results that we
343 anticipated), which can at best yield a set of trees showing where the extinct taxa most
344 parsimoniously fit (if we had dozens of characters, this might be feasible). Comparisons with
345 other hypotheses through direct phylogenetic analysis are not possible. Given the small
346 sample size (which here is the number of characters), we computed the corrected AIC (AICc)
347 and the AICc weights using the formulae given by Anderson and Burnham (2002) and
348 Wagenmakers and Farrell (2004).

349 Our tests make sense only in the presence of a phylogenetic signal in the data. In
350 addition to the test of evolutionary model in CoMET evoked above (which tests non-
351 phylogenetic as well as phylogenetic models), we performed a test based on squared-change
352 parsimony (Maddison 1991) and random taxon reshuffling (Laurin 2004). For this test, we
353 compared the length of the LH (lepospondyl hypothesis; Fig. 1d) reference tree (with and
354 without *Sclerocephalus*) to a population of 10,000 random trees produced by taxon
355 reshuffling.

356 It could be argued that using other methods (in addition to the method outlined above)
357 would have facilitated comparisons with previous studies. However, the two main alternative

358 methods, event-pair cracking with Parsimov (Jeffery et al. 2005) and Parsimov-based genetic
359 inference (PGI; Harrison and Larsson 2008), have drawbacks that decided us against using
360 them. Our objections against event-pair cracking with Parsimov were detailed by Germain
361 and Laurin (2009) but can be summarized briefly as including the unnecessary decomposition
362 of sequences into event pairs and the fact that the method cannot incorporate absolute timing
363 information (in the form of time, developmental stage or body size, for instance) or branch
364 length information. More importantly, the simulations performed by Germain and Laurin
365 (2009) showed that event-pair cracking with Parsimov yields more artefactual change and has
366 lower power to detect real sequence shifts. That method is also problematic when trying to
367 infer ancestral sequences and can lead to impossible ancestral reconstructions (e.g. A occurs
368 before B, B occurs before C, and C occurs before A), as had been documented previously.
369 This would create problems when trying to compare the fit of the data on various
370 phylogenetic hypotheses. The performance of Parsimov-based genetic inference (PGI;
371 Harrison and Larsson 2008) has not been assessed by simulations, but it rests on an edit cost
372 function that is contrary to our working hypothesis (that the timing of developmental events
373 can be modeled with a bounded Brownian motion model, which is assumed by continuous
374 analysis). More specifically, Harrison and Larsson (2008: 380) stated that their function
375 attempts to minimize the number of sequence changes, regardless of the magnitude of these
376 changes. We believe that disregarding the size of changes is unrealistic, as shown by the fact
377 that Poe's (2006) analyses of thirteen empirical datasets rejected that model (which he called
378 UC, for unconstrained change) in favor of the model we accept (AJ for adjacent states, which
379 favors small changes over large ones). Furthermore, analyses of ossification sequence data
380 using techniques for continuous data as done here (see above) have been performed by an
381 increasingly large number of studies (e.g., Skawiński and Borczyk 2017; Spiekman and
382 Werneburg 2017; Werneburg and Geiger 2017, just to mention papers published in 2017), so

383 the issue of ease of comparisons of our results with other studies is not as serious as it would
384 have been only a few years ago, and it should be decreasingly so in the future.

385 *Reference phylogenies*

386 We built a reference timetree that attempts to capture the established consensus (Fig. 2). The
387 tree was compiled in Mesquite versions up to 3.6 (Maddison and Maddison 2018) and time-
388 calibrated using the Stratigraphic Tools module for Mesquite (Josse et al. 2006). For
389 consistency and to avoid the effects of gaps in the fossil record, we used molecular divergence
390 dates whenever possible. The tree had to be time-scaled because many of the evolutionary
391 models that we fit on the tree in the first series of tests (to determine which evolutionary
392 model can be used to compare the fit of the hypotheses) use branch lengths to assess model
393 fit. Note that our procedure requires estimating divergence times between all taxa (geological
394 ages of all nodes). When taxa are pruned, branch lengths are adjusted automatically. The main
395 sources we used for topology and divergence times (and hence branch lengths) are as follows:

396 The phylogeny of lissamphibians follows the work of Jetz and Pyron (2018).
397 However, several other sources have been used for the temporal calibration of the tree:
398 Germain and Laurin (2009) was used for the urodeles, whereas Feng et al. (2017),
399 supplemented by Bossuyt and Roelants (2009) and Pyron (2014), was used for the anurans as
400 well as more rootward nodes (Batrachia, Lissamphibia, Tetrapoda; also Amniota). Marjanović
401 and Laurin (2014) was used for the Ranidae, Ceratophryidae and Hylidae.

402 The sediments that have preserved the temnospondyls *Apateon* and *Sclerocephalus* are
403 not easy to correlate with each other or with the global chronostratigraphic scale. Combining
404 stratigraphic information from Schoch (2014a), Schneider et al. (2015) and Werneburg
405 (2018), we have placed all three sampled species (*A. pedestris*, *A. caducus*, *S. haeuseri*) at the
406 Sakmarian/Artinskian stage boundary (Permian; 290.1 Ma ago); combining stratigraphic

407 information from Schneider et al. (2015) with the phylogeny in Schoch (2014a), we have
408 tentatively placed the divergence between the two *Apateon* species (which are not sister-
409 groups: Schoch 2014a) at the Kasimovian/Gzhelian stage boundary (Carboniferous; 303.7 Ma
410 ago). The age of the last common ancestor of *Apateon* and *Sclerocephalus* depends strongly
411 on temnospondyl phylogeny, which remains unresolved (Pardo et al. 2017b; Marjanović and
412 Laurin 2019; and numerous references in both); as a compromise between the various options,
413 we have provisionally placed it at the boundary between the Early and the Late Carboniferous
414 (Serpukhovian/Bashkirian, 323.2 Ma ago) where applicable.

415 For the birds, Pons et al. (2005) was used for the Laridae, Wang et al. (2013) for the
416 Phasianidae and Gonzales et al. (2009) for the Anatidae. The temporal calibration was taken
417 from Prum et al. (2015) as recommended by Berv and Field (2017); gaps were filled in using
418 the database www.birdtree.org.

419 Several papers, mainly Tarver et al. (2016), were used for the phylogeny and
420 divergence times of mammals. For the Muridae, three references were used: Lecompte et al.
421 (2008), Zhuang et al. (2015), and Lu et al. (2017) for the position of two taxa: *Mesocricetus*
422 *auratus* and *Peromyscus melanophrys*. Other species were placed following the work of
423 Meredith et al. (2011), which also gives divergence times. We caution, however, that all
424 available molecular dates for Paleogene and earlier mammal nodes are controversial and may
425 be overestimates (Berv and Field 2017).

426 Three references were also used to integrate squamates in the phylogenetic tree and for
427 the calibration of divergence times: Brandley et al. (2005), Rabosky et al. (2014), Reeder
428 (2003). Sterli et al. (2013) was used for turtles.

429 For turtles, there is now a near-consensus that they are diapsids, a hypothesis that is
430 not necessarily incompatible with an origin among “parareptiles” (Laurin and Piñeiro 2017).

431 Thus, following most recent molecular phylogenetic analyses (e.g., Hugall et al. 2007; Irisarri
432 et al. 2017), we have inserted them as the sister-group of Archosauria.

433 We disagree with several of the calibration dates in Irisarri et al. (2017), which often
434 appear unreasonably old. For instance, they place the divergence between caecilians and
435 batrachians and the divergence between anurans and urodeles in the Early Carboniferous,
436 around 330 and 320 Ma, respectively, but our thorough analyses of the fossil record, with due
437 consideration of its incompleteness, suggest significantly more recent dates, in the Permian
438 (Marjanović and Laurin 2007, 2008, 2014). This is not surprising because some of the dating
439 constraints used by Irisarri et al. (2017: table S8) are wrong. For instance, they enforced a
440 minimal divergence age between cryptodiran and pleurodiran turtles of 210 Ma (Late
441 Triassic), but all analyses of the last fifteen years (e.g. Sterli et al. 2013, 2018) strongly
442 suggest that the oldest known turtles that fit within this dichotomy date from the Late Jurassic,
443 less than 165 Ma. The divergence between humans and armadillos (boreotherian and
444 xenarthran placentals) was constrained to the middle of the Cretaceous (95.3–113 Ma), based
445 on outdated literature that assigned a wide variety of stem-eutherians to highly nested
446 positions in the placental crown; there are currently no clear placentals known from any
447 Cretaceous sediments even as young as 66 Ma (see e.g. Wible et al. 2009), barely half the age
448 of the older end of the constraint range. Conversely, the divergence between diapsids (hence
449 sauropsids) and synapsids had a minimal age constraint of 288 Ma (Early Permian), which is
450 much too young given the presence of sauropsids (and presumed synapsids) in Joggins, in
451 sediments that have recently been dated (Carpenter 2015) around 317–319 Ma (early Late
452 Carboniferous). Thus, we have not used divergence dates from that source.

453 To discriminate among the hypotheses on lissamphibian origins, we inserted the
454 temnospondyl *Apateon* in the tree where each predicts that it should be (Fig. 1c–h). Thus,
455 according to the TH (temnospondyl hypothesis; Fig. 1c), *Apateon* lies on the lissamphibian

456 stem. Under the LH (lepospondyl hypothesis; Fig. 1d), *Apateon* lies on the tetrapod stem.
457 Under both versions of the DH (diphyly hypothesis; Fig. 1g, h), *Apateon* lies on the
458 batrachian stem. Under both versions of the PH (polyphyly hypothesis; Fig. 1e, f), *Apateon*
459 lies on the caudate stem. Within the DH and the PH, both versions of each differ in the
460 position of Gymnophiona. Thus, despite the absence of any lepospondyl in our cranial
461 ossification sequence dataset, our taxonomic sample allows us to test all these competing
462 hypotheses. The appendicular datasets allow more direct tests of some of these hypotheses
463 because they include two lepospondyl taxa, which were likewise placed in trees representing
464 the tested hypotheses (Fig. 1).

465 *Sclerocephalus* is the sister-group of *Apateon* under the LH (Fig. 1d), immediately
466 rootward of it (on the lissamphibian stem) under the TH (Fig. 1c) and likewise (but on the
467 batrachian stem) under the DH1 (Fig. 1g), on the caecilian stem under the DH2 (Fig. 1h) and
468 the sister-group of Batrachia (including *Apateon*) under both versions of the PH (Fig. 1e, f).

469 “*Melanerpeton*” *humbergense* (appendicular data only) is the sister-group of *Apateon*
470 in all trees, except under the hypothesis of branchiosaur paraphyly; *Eusthenopteron*
471 (appendicular data only) forms the outgroup in all trees.

472 The lepospondyls *Microbrachis* and *Hyloplesion*, from both of which only
473 appendicular data are available, form an exclusive clade (Marjanović and Laurin 2019; Clack
474 2019). This clade is the sister-group of Lissamphibia (represented only by Batrachia) under
475 the LH (because caecilians are lacking from the appendicular datasets), of Amniota under the
476 TH and both versions of the DH (these three cannot be distinguished due to the absence of
477 caecilians) as well as under the PH1, and of Temnospondyli (including Batrachia) under the
478 PH2.

479 The temnospondyl *Micromelerpeton*, from which likewise only appendicular data are
480 available, forms the sister-group of *Apateon* under the LH. The uncertainty over its
481 phylogenetic position within Dissorophoidea (as the sister-group to the rest, including anurans
482 and urodeles: e.g. Schoch 2019; as the sister-group of *Apateon* + “*Melanerpeton*”
483 *humbergense*: e.g. Ruta & Coates 2007; Marjanović and Laurin 2019) generates two versions
484 of the TH/DH1/DH2 tree for the appendicular dataset. We tested both of these versions
485 against that dataset, for a total of five trees.

486 To ensure that our analyses were not biased in favor of a given hypothesis, and in case
487 that a continuous evolutionary model were favored, we initially adjusted the branch lengths
488 such that the sum of branch lengths was equal between the compared topologies and that the
489 root was approximately at the same age (in this case in the Tournaisian, the first stage of the
490 Carboniferous). This was done for the trees used to compare the hypotheses using the cranial
491 dataset because if a model incorporating (variable) branch length information had been
492 selected, and if the trees representing the various hypotheses had not all had the same total
493 length (the sum of all branch lengths), the resulting distortions in branch lengths created
494 around the extinct taxa (whose height compared to extant taxa is specified by their geological
495 age) would have introduced another variable influencing the AICc. But given that the selected
496 model ignores branch lengths, this precaution turned out to be superfluous. We have therefore
497 not made these time-consuming adjustments to the additional trees we generated later to
498 analyze the appendicular data.

499 RESULTS

500 In the phylogenetic analysis of cranial data, a single tree island of 22,077 trees of 438 steps
501 was found, only once, so there might be more trees of that length and perhaps even shorter
502 trees. Initially, an island of 22,075 trees was found; we swapped on each of these in a

503 subsequent run, which only recovered two additional trees. Given that slightly longer trees did
504 not differ much from those that we obtained, the low quality of the results (poor congruence
505 with the established consensus about the monophyly of major clades such as squamates, birds,
506 mammals and turtles) and the fact that about four full days of computer time had been spent
507 on analysis of the cranial data, we did not pursue that search further. As expected, the strict
508 consensus tree is poorly resolved (Fig. 3). For the appendicular matrix, 22,757 trees of 164
509 steps were found. Their strict consensus (Fig. 4) deviates even more from the established
510 consensus than the tree obtained from cranial data.

511 This visual assessment of phylogenetic signal through an examination of the
512 consensus trees (Figs. 3, 4) is congruent with the test based on squared-change parsimony and
513 random taxon reshuffling (Laurin 2004). Indeed, the latter indicates that the phylogenetic
514 signal in the cranial data is fairly strong, with a probability of less than 0.0001 that the
515 observed covariation between the data and the tree reflects a random distribution (none of the
516 10,000 random trees generated were as short as the reference tree), but it is weaker, with a
517 probability of 0.0017, for the appendicular data.

518 The speciation model of evolution, in which all branch lengths are equal, has
519 overwhelming support among cranial data, whether or not the Permian temnospondyl
520 *Sclerocephalus* (Table 2) or the squamosal (Table 3) are included (including *Sclerocephalus*
521 adds a second temnospondyl genus, but given that the timing of ossification of the squamosal
522 is unknown in *Sclerocephalus*, including it requires excluding the squamosal from the
523 analysis); the five other examined models have AICc weights $< 10^{-11}$. For the appendicular
524 data, the speciation model also has the most support, but that support is not as strong and
525 varies depending on which dataset is analyzed (seven characters or four) and under which
526 phylogenetic hypothesis. In three of the four tests performed, support for the second-best
527 model, the non-phylogenetic/equal model, varied between 5% and 19% (Table 4).

528 Two main conclusions can be drawn from these tests (Tables 2–4). First, given that
529 both of the best-supported models imply equal branch lengths, actual time represented by
530 branches can be ignored, so we compare support of the six competing topologies using only
531 the best-supported model (speciational). This simplifies the discussion, because it means that
532 the original branch lengths are irrelevant (under that model, all branch lengths are equal);
533 unfortunately, the branch length (evolutionary time) data were needed to reach this
534 conclusion. Thus, the only remaining variable is the topology. Second, model fitting, along
535 with the test based on squared-change parsimony and random taxon reshuffling, indicates that
536 the phylogenetic signal in the cranial data is strong, but that it is noticeably weaker in the
537 appendicular data (this is shown mostly by the non-negligible support for the non-
538 phylogenetic/equal model). Thus, comparisons of the fit of the various phylogenetic
539 hypotheses for the cranial data should be more reliable than for the appendicular data.
540 However, given that for several Paleozoic taxa (most importantly both of the sampled
541 lepospondyls), comparisons can be performed only for the appendicular data, these were
542 performed as well.

543 Using the speciational model, the AICc weights of the six compared topologies
544 indicate that there is strong support in the cranial data for the LH (lepospondyl hypothesis),
545 with an AICc weight of 0.9885 when *Sclerocephalus* is included (Table 5) and 0.8848 when
546 the squamosal is included instead (Table 6). Of the other topologies, the TH (temnospondyl
547 hypothesis) was by far the best supported, with an AICc weight of 0.01144 (with
548 *Sclerocephalus*) or 0.1056 (with the squamosal), which is 86.44 or 8.38 times less than for the
549 LH. Both versions of the DH (diphyly hypothesis) and of the PH (polyphyly hypothesis) have
550 negligible support (AICc weights < 0.01 when the squamosal is included, < 0.0001 when
551 *Sclerocephalus* is included). The least support is found for the PH2 when *Sclerocephalus* is
552 included, and for the DH1 when the squamosal is included. In both cases, the recently

553 proposed DH2 (Pardo et al. 2017b) fares second-worst by a small margin. Notably, the DH1
554 contradicts the modern consensus on lissamphibian monophyly (Fig. 1g), while the PH2 and
555 the DH2 fulfill this constraint from the molecular but not the paleontological point of view,
556 having lissamphibian monophyly with respect to amniotes but not with respect to
557 temnospondyls (Fig. 1f, h).

558 A slightly different dataset is used (only 84 taxa, but eight cranial characters, the
559 additional one being the frontal, and *Apateon* sequences for both species from Erdesbach
560 rather than Obermoschel) provides even stronger support for the LH, with an AICc weight of
561 0.9935 (Table 7). The next best-supported topology, which simultaneously represents the TH,
562 DH1 and DH2, has an AICc weight of only 0.0065.

563 The appendicular data are available in far more Paleozoic taxa than the cranial data;
564 these include *Sclerocephalus haeuseri*, *Archegosaurus decheni*, and the non-branchiosaurid
565 “branchiosaur” *Micromelerpeton credneri* among temnospondyls, the lepospondyls
566 *Hyloplezion longicaudatum* and *Microbrachis pelikani*, and the tristichopterid finned stem-
567 tetrapodomorph *Eusthenopteron foordi*, in addition to the same two species of *Apateon* as for
568 the cranial datasets, *A. caducus* and *A. pedestris*. Analysis of these postcranial data (seven
569 characters: humerus, radius, ulna, ilium, femur, tibia and fibula) yields surprising results, with
570 the PH2 having the most support, with an AICc weight of 0.7978 when using the dataset of
571 seven bones (Table 8). The TH, DH1 and DH2 with “branchiosaur” monophyly are
572 collectively (they cannot be distinguished with that taxonomic sample) the second-best
573 hypotheses with that dataset, with an AICc weight of only 0.1874. The least-supported
574 hypothesis with these data is the TH with “branchiosaur” polyphyly.

575 Using the other postcranial dataset with only four bones (radius, ulna, ilium, and
576 femur) but with more taxa (notably the branchiosaurid temnospondyl “*Melanerpeton*”

577 *humbergense*) shows that infraspecific variation in the postcranial ossification sequences of
578 *Apateon* do not significantly impact our assessment of the support for various hypotheses.
579 Whether both sequences of *Apateon* (from the Erdesbach and Obermoschel localities) are
580 included (treated as if they were distinct taxa, such as subspecies), or whether either one of
581 these is used in isolation, the PH2 retains the highest support, with AICc weights of 0.62 to
582 0.65. The LH is a distant second, at 0.20–0.23, but still well ahead of the TH/DH and the PH1,
583 which all receive AICc weights between 0.03 and 0.06 (Table 9).

584 DISCUSSION

585 *Phylogenetic signal*

586 In his discussion of previous phylogenetic conclusions from ossification sequences (e.g.
587 Schoch and Carroll 2003), Anderson (2007) noted that ossification sequences seemed to
588 abound in symplesiomorphies and in autapomorphies of terminal taxa, while potential
589 synapomorphies were scarce. This pessimism was seemingly confirmed by Schoch (2006) in
590 a paper that was published after Anderson's (2007) book chapter had gone to press: not only
591 were many similarities in the cranial ossification sequences across Osteichthyes found to be
592 symplesiomorphies, but a phylogenetic analysis of cranial ossification sequences did not
593 recover Mammalia, Sauropsida, Amniota or Lissamphibia as monophyletic. Along with these
594 results, Schoch (2006) dismissed another: the position of the temnospondyl *Apateon caducus*
595 (the only included extinct taxon) outside the tetrapod crown-group, i.e. the lepospondyl
596 hypothesis on lissamphibian origins (LH).

597 While ossification sequences alone may not provide enough data for a phylogenetic
598 analysis, as shown by our results (Fig. 3, 4), our datasets (with much larger taxon samples
599 than in Schoch 2006) fit some tree topologies much better than others. Both the tests using
600 CoMET and squared-change parsimony with random taxon reshuffling overwhelmingly

601 support the presence of a strong phylogenetic signal in the cranial data; the null hypothesis of
602 the absence of a phylogenetic signal can be rejected in both cases, given that it has a
603 probability of $< 10^{-97}$ for the cranial and $< 10^{-4}$ for the appendicular dataset. We conclude that
604 the cranial dataset contains a strong phylogenetic signal, and are therefore cautiously
605 optimistic about future contributions of ossification sequences to phylogenetics. We are less
606 optimistic about the appendicular sequence data, which both tests suggest contains less
607 phylogenetic signal.

608 The sizable effect on nodal estimates and inferred heterochronies of infraspecific
609 variation found by Sheil et al. (2014) in lissamphibians could raise doubts about the
610 robustness of our findings. We have been able to incorporate infraspecific variability in only
611 two terminal taxa (*Apateon caducus* and *A. pedestris*), but *Apateon* has played a prominent
612 role in discussions about the significance of cranial ossification sequences on the origins of
613 extant amphibians (Schoch and Carroll 2003; Schoch 2006; Germain and Laurin 2009). Thus,
614 incorporation of infraspecific variability in *Apateon* is presumably much more important than
615 in extant taxa, even though variability in the latter would obviously add to the analysis and
616 should be tackled in the future. The variability in *Apateon* should be exempt from two sources
617 of artefactual variability in ossification sequences discussed by Sheil et al. (2014), namely the
618 way in which the specimens were collected (there can be no lab-raised specimens in long-
619 extinct taxa) and the fixing method used (in this case, fossilization under quite consistent
620 taphonomic conditions). The finding that whether we used the *Apateon* sequences from
621 Erdesbach, Obermoschel, or both, we find very similar results (Table 9), is reassuring. In this
622 case, infraspecific variation has negligible impact. However, future studies should attempt to
623 assess the effect of more generalized incorporation of infraspecific variability (in a greater
624 proportion of the OTUs).

625 Of course, these results do not preclude functional or developmental constraints from
626 applying to the same data. This phenomenon has been documented, among other taxa, in
627 urodeles, whose development has often been compared with that of temnospondyls (e.g.
628 Schoch 2006; Schoch and Carroll 2003; Fröbisch et al. 2007, 2015; Germain and Laurin
629 2009). For instance, Vorobyeva and Hinchliffe (1996) documented the larval functional
630 constraints linked to early forelimb use that may cause an early development of manual digits
631 1 and 2, compared with other tetrapods, as briefly discussed below. However, in the case of
632 our seven cranial characters, there is no evidence of functional constraints. This is a little-
633 investigated topic, but all these bones apparently form a single developmental module of the
634 urodele skull (Laurin 2014). For the appendicular data, functional constraints might explain
635 the more subdued phylogenetic signal, but this will have to be determined by additional
636 research.

637 The finding that the postcranial characters that we analyzed contain relatively little
638 phylogenetic signal may raise doubts about the claims that have been made about the
639 phylogenetic implications of other such data. Specifically, Carroll et al. (1999) stated that the
640 neural arches ossify before the centra in frogs and temnospondyls, but not in salamanders,
641 caecilians or lepospondyls. When it was found that the centra do ossify first in a few
642 cryptobranchoid salamanders, Carroll (2007: 30) took this as “strong evidence that the most
643 primitive crown-group salamanders had a sequence of vertebral development that is common
644 to frogs and labyrinthodonts (but distinct from that of lepospondyls)”. In fact, apart from tail
645 regeneration in *Hyloplestion* and *Microbrachis* (where the centra ossify before the neural
646 arches: Olori 2015; Fröbisch et al. 2015; van der Vos et al. 2017), only one incompletely
647 ossified vertebral column (referred to *Utaherpeton*) is known of any putative lepospondyl. “In
648 this specimen, [...] five neural arches [...] have ossified behind the most posterior centrum.”

649 (Carroll and Chorn 1995: 40–41) Carroll’s (2007: 85) claim that “the centra always ossified
650 prior to the arches” in lepospondyls is therefore rather puzzling.

651 Fröbisch et al. (2007, 2015) pointed out that the first two digital rays (digits,
652 metapodials and distal carpals/tarsals) ossify before the others (“preaxial polarity”) in
653 salamanders and the temnospondyls *Apateon*, *Micromelerpeton* and *Sclerocephalus*, while the
654 fourth ossifies first (“postaxial polarity”) in amniotes, frogs and “probably” (Fröbisch et al.
655 2015: 233, 234) the lepospondyls *Microbrachis* and *Hyloplezion*. This latter inference,
656 however, is based only on a delay in the ossification of the fifth ray that is shared specifically
657 with sauropsid amniotes (Olori 2015). Ossification sequences (however partial) of the other
658 four rays in any lepospondyl are currently limited to the tarsus of *Batropetes*, which clearly
659 shows preaxial polarity (Gliénke 2015: fig. 6O–S; Marjanović and Laurin 2019), and that of
660 the putative (but see Clack et al. 2019) lepospondyl *Sauroplorea*, in which likewise the
661 second distal tarsal ossified before all others (Marjanović and Laurin 2019). Outside of
662 temno- and lepospondyls, Marjanović and Laurin (2013, 2019) presented evidence that
663 preaxial polarity is plesiomorphic, widespread and dependent on the use of the still
664 developing limbs for locomotion, which would explain why it was independently lost in
665 amniotes and frogs and reduced (the third ray ossifies first) in direct-developing salamanders.
666 It may be relevant here that the PH2 (Fig. 1f), favored by our appendicular data, groups
667 exactly those sampled taxa in a clade that are known to have preaxial polarity in limb
668 development. To sum up, neither our own analyses nor the previous works that we cited
669 above demonstrated conclusively that ossification sequences of postcranial elements provide
670 reliable clues about the origin of extant amphibians.

671 In contrast, we are reasonably confident about our results on the cranial ossification
672 sequences. Given the phylogenetic signal we have found in our cranial datasets, we think that
673 ossification sequence data should eventually be added to phenotypic datasets for analyses of

674 tetrapod phylogeny. Indeed, an analysis of amniote phylogeny using data from organogenesis
675 sequences (coded using event-pairing in Parsimov) already exists (Werneburg and Sánchez-
676 Villagra 2009). The usefulness of such data for phylogenetic inference was further tested,
677 with encouraging results, by Laurin and Germain (2011), and the present analysis adds
678 additional support for it.

679 *Indirect support for the lepospondyl hypothesis from temnospondyls*

680 The strong support for the lepospondyl hypothesis that we have found in cranial data is
681 surprising because cranial ossification sequence data, especially those of the Permo-
682 Carboniferous temnospondyl *Apateon*, have often been claimed to contradict the LH
683 (lepospondyl hypothesis, Fig. 1d). Similarities between *Apateon* and extant urodeles, in
684 particular the supposedly “primitive” hynobiid *Ranodon*, have often been emphasized
685 (Schoch and Carroll 2003; Schoch and Milner 2004; Carroll 2007; Schoch 2014b). However,
686 other studies have already raised doubts about some of these claims (e.g. Schoch 2006;
687 Anderson 2007; Germain and Laurin 2009). Schoch (2006) and Anderson (2007) concluded
688 that most characters shared between *Apateon* and urodeles were plesiomorphies. Germain and
689 Laurin (2009) also demonstrated that, far from being very similar to the ancestral urodele
690 morphotype (contra Schoch and Carroll 2003 or Carroll 2007), the cranial ossification
691 sequence of *Apateon* was statistically significantly different from that of the hypothetical last
692 common ancestor of all urodeles (as suspected by Anderson 2007). However, these earlier
693 studies did not clearly show which of the various hypotheses on lissamphibian origins the
694 ossification sequences of *Apateon* spp. – or the newly available partial sequence (Werneburg
695 2018) of the phylogenetically distant temnospondyl *Sclerocephalus* – supported most. This is
696 what we have attempted to do here.

697 Unfortunately, the development of lepospondyls is too poorly documented to be
698 incorporated into the cranial analyses, but we included two lepospondyls in analyses of
699 appendicular data. These analyses weakly favor a polyphyletic origin of extant amphibians,
700 with both temno- and lepospondyls in the amphibian clade, a hypothesis that has not been
701 advocated seriously for decades (Milner 1993: fig. 5B) as far as we know. However, given the
702 moderate phylogenetic signal in these data, we view these results with skepticism. Olori
703 (2011), using event-pairing with Parsimov (Jeffery et al. 2005) and PGi (Harrison and Larsson
704 2008), analyzed lepospondyl postcranial ossification sequences and concluded that support for
705 the three hypotheses that she tested (TH/DH with two different positions for
706 *Micromelerpeton*, and LH) did not differ significantly. By contrast, our analyses of the
707 postcranial data indicate a stronger support for polyphyly (PH2) than for the TH/DH, which is
708 only a distant second (Table 8) or third (behind PH2 and LH; Table 9) depending on the
709 analyses. Olori (2011) performed no statistical test of phylogenetic signal of her data, though
710 a related test (performing phylogenetic analyses on the data) yielded trees (Olori, 2011: fig.
711 5.5–5.7) that are largely incongruent with the established consensus, in which most large taxa
712 (Mammalia, Testudines, Lissamphibia, etc.) are para- or polyphyletic. Olori's (2011) results,
713 like ours, support the conclusion that the phylogenetic signal in postcranial ossification
714 sequence data is low.

715 Given the current limitations in the availability of developmental data in Paleozoic
716 stegocephalians, we hope to have demonstrated that cranial ossification sequences of
717 amniotes, lissamphibians and temnospondyls provide support for the LH that is independent
718 of the phylogenetic analyses of Laurin (1998), Pawley (2006: appendix 16) or Marjanović and
719 Laurin (2009, 2018). This independence is important because the cranial ossification sequence
720 data cannot rival the morphological data in terms of data availability, simply because growth
721 sequences of extinct taxa are rare (Sánchez-Villagra 2012), but having a fairly independent

722 line of evidence to investigate a major evolutionary problem is clearly advantageous. We
723 hope that the modest methodological progress made in this study will stimulate the search for
724 fossilized ontogenies (Cloutier 2009; Sánchez-Villagra 2010).

725 FUNDING

726 This work was supported by the Centre National de la Recherche Scientifique and the French
727 Ministry of Research (unnumbered recurring grants to the CR2P, for ML).

728 ACKNOWLEDGEMENTS

729 Jennifer Olori, two anonymous reviewers and the editor Robert Asher made helpful comments
730 that improved this paper. D. M. would further like to thank Ralf Werneburg for an electronic
731 reprint of his 2018 paper, and Daniel Field for discussion of molecular divergence times and
732 the fossil record.

733

734 REFERENCES

- 735 Anderson J.S. 2007. Incorporating ontogeny into the matrix: a phylogenetic evaluation of
736 developmental evidence for the origin of modern amphibians. Pages 182–227 in
737 Anderson J.S., Sues H.-D., editors. Major transitions in vertebrate evolution.
738 Bloomington: Indiana University Press.
- 739 Anderson D.R., Burnham K.P. 2002. Avoiding pitfalls when using information-theoretic
740 methods. *J. Wildl. Manag.* 66:912–918.
- 741 Anderson J.S., Carroll R.L., Rowe T.B. 2003. New information on *Lethiscus stocki*
742 (Tetrapoda: Lepospondyli: Aistopoda) from high-resolution computed tomography and
743 a phylogenetic analysis of Aistopoda. *Can. J. Earth Sci.* 40:1071–1083.
- 744 Anderson J.S., Reisz R.R., Scott D., Fröbisch N.B., Sumida S.S. 2008. A stem batrachian
745 from the Early Permian of Texas and the origin of frogs and salamanders. *Nature*
746 453:515–518.
- 747 Berv J.S., Field D.J. 2017 (printed 2018). Genomic signature of an avian Lilliput Effect across
748 the K-Pg Extinction. *Syst. Biol.* 67:1–13.
- 749 Bolt J.R. 1969. Lissamphibian origins: possible protolissamphibian from the Lower Permian
750 of Oklahoma. *Science* 166:888–891.
- 751 Bossuyt F., Roelants K. 2009. Frogs and toads (Anura). Pages 357–364 in Hedges S.B.,
752 Kumar S., editors. *The Timetree of Life*. New York: Oxford University Press.
- 753 Brandley M.C., Schmitz A., Reeder T.W. 2005. Partitioned Bayesian analyses, partition
754 choice, and the phylogenetic relationships of scincid lizards. *Syst. Biol.* 54:373–390.
- 755 Carpenter D.K., Falcon-Lang H.J., Benton M.J., Grey M. 2015. Early Pennsylvanian
756 (Langsettian) fish assemblages from the Joggins Formation, Canada, and their
757 implications for palaeoecology and palaeogeography. *Palaeontology* 58:661–690.

- 758 Carroll R.L. 2001. The origin and early radiation of terrestrial vertebrates. *J. Paleontol.*
759 75:1202–1213.
- 760 Carroll R.L. 2007. The Palaeozoic ancestry of salamanders, frogs and caecilians. *Zool. J.*
761 *Linn. Soc.* 150 (suppl. 1):1–140.
- 762 Carroll R.L., Chorn J. 1995. Vertebral development in the oldest microsauro and the problem
763 of “lepospondyl” relationships. *J. Vert. Paleont.* 15:37–56.
- 764 Carroll R.L., Currie P.J. 1975. Microsaurs as possible apodan ancestors. *Zool. J. Linn. Soc.*
765 57:229–247.
- 766 Carroll R.L., Holmes R. 1980. The skull and jaw musculature as guides to the ancestry of
767 salamanders. *Zool. J. Linn. Soc.* 68:1–40.
- 768 Carroll R.L., Kuntz A., Albright K. 1999. Vertebral development and amphibian evolution.
769 *Evol. Dev.* 1:36–48.
- 770 Cope E.D. 1888. On the intercentrum of the terrestrial Vertebrata. *Trans. Am. Phil. Soc.*
771 16:243–253.
- 772 Cloutier R. 2009 (printed 2010). The fossil record of fish ontogenies: Insights into
773 developmental patterns and processes. *Semin. Cell Dev. Biol.* 21:400–413.
- 774 Danto M., Witzmann F., Kamenz S., Fröbisch N. 2019. How informative is vertebral
775 development for the origin of lissamphibians? *J. Zool. (Lond.)* 307:292–305.
- 776 Eldredge N., Gould S.J. 1972. Punctuated equilibria: an alternative to phyletic gradualism.
777 Pages 82–115 in Schopf T.J.M., editor. *Models in Paleobiology*. San Francisco:
778 Freeman, Cooper & Company.
- 779 Feng Y.-J., Blackburn D.C., Liang D., Hillis D.M., Wake D.B., Cannatella D.C., Zhang P.
780 2017. Phylogenomics reveals rapid, simultaneous diversification of three major clades
781 of Gondwanan frogs at the Cretaceous–Paleogene boundary. *Proc. Natl. Acad. Sci. USA*
782 E5864–E5870.

- 783 Fröbisch N.B., Carroll R.L., Schoch R.R. 2007. Limb ossification in the Paleozoic
784 branchiosaurid *Apateon* (Temnospondyli) and the early evolution of preaxial dominance
785 in tetrapod limb development. *Evol. Dev.* 9:69–75.
- 786 Fröbisch N.B., Bickelmann C., Olori J.C., Witzmann F. 2015. Deep-time evolution of
787 regeneration and preaxial polarity in tetrapod limb development. *Nature* 527:231–234.
- 788 Germain D., Laurin M. 2009. Evolution of ossification sequences in salamanders and urodele
789 origins assessed through event-pairing and new methods. *Evol. Dev.* 11:170–190.
- 790 Glienke S. 2015. Two new species of the genus *Batropetes* (Tetrapoda, Leptospondyli) from
791 the Central European Rotliegend (basal Permian) in Germany. *J. Vert. Paleont.*
792 35:e918041.
- 793 Gonzalez J., Düttmann H., Wink M. 2009. Phylogenetic relationships based on two
794 mitochondrial genes and hybridization patterns in Anatidae. *J. Zool.* 279:310–318.
- 795 Harrington S.M., Harrison L.B., Sheil C.A. 2013. Ossification sequence heterochrony among
796 amphibians. *Evol. Dev.* 15:344–364.
- 797 Harrison L.B., Larsson H.C.E. 2008. Estimating evolution of temporal sequence changes: a
798 practical approach to inferring ancestral developmental sequences and sequence
799 heterochrony. *Syst. Biol.* 57:378–387.
- 800 Hugall A.F., Foster R., Lee M.S.Y. 2007. Calibration choice, rate smoothing, and the pattern
801 of tetrapod diversification according to the long nuclear gene RAG-1. *Syst. Biol.*
802 56:543–563.
- 803 Hugi J., Hutchinson M.N., Koyabu D., Sánchez-Villagra M.R. 2012. Heterochronic shifts in
804 the ossification sequences of surface- and subsurface-dwelling skinks are correlated with
805 the degree of limb reduction. *Zoology* 115:188–198.

- 806 Irisarri I., Baurain D., Brinkmann H., Delsuc F., Sire J.-Y., Kupfer A., Petersen J., Jarek M.,
807 Meyer A., Vences M., Philippe H. 2017. Phylotranscriptomic consolidation of the jawed
808 vertebrate timetree. *Nature Ecol. Evol.* 1:1370–1378.
- 809 Jeffery J.E., Bininda-Emonds O.R.P., Coates M.I., Richardson M.K. 2005. A new technique
810 for identifying sequence heterochrony. *Syst. Biol.* 54:230–240.
- 811 Jetz W., Pyron R.A. 2018. The interplay of past diversification and evolutionary isolation
812 with present imperilment across the amphibian tree of life. *Nat. Ecol. Evol.* 2:850–858.
- 813 Josse S., Moreau T., Laurin M. 2006. Stratigraphic tools for Mesquite, version 1.0.
814 <http://mesquiteproject.org/packages/stratigraphicTools/>
- 815 Koyabu D., Werneburg I., Morimoto N., Zollikofer C.P.E., Forasiepi A.M., Endo H., Kimura
816 J., Ohdachi S.D., Son N.T., Sánchez-Villagra M.R. 2014. Mammalian skull
817 heterochrony reveals modular evolution and a link between cranial development and
818 brain size. *Nat. Commun.* 5:3625.
- 819 Laurin M. 1998. The importance of global parsimony and historical bias in understanding
820 tetrapod evolution. Part I. Systematics, middle ear evolution, and jaw suspension. *Ann.*
821 *Sci. Nat., Zool., 13^e Sér.* 19:1–42.
- 822 Laurin M. 2004. The evolution of body size, Cope's rule and the origin of amniotes. *Syst.*
823 *Biol.* 53:594–622.
- 824 Laurin M. 2014. Assessment of modularity in the urodele skull: an exploratory analysis using
825 ossification sequence data. *J. Exp. Zool. B (Mol. Dev. Evol.)* 322:567–585.
- 826 Laurin M., Germain D. 2011. Developmental characters in phylogenetic inference and their
827 absolute timing information. *Syst. Biol.* 60:630–644.
- 828 Laurin M., Piñeiro G. 2017. A reassessment of the taxonomic position of mesosaurs, and a
829 surprising phylogeny of early amniotes. *Front. Earth Sci.* 5:88.
- 830 Lecompte E., Aplin K., Denys C., Catzeflis F., Chades M., Chevret P. 2008. Phylogeny and

- 831 biogeography of African Murinae based on mitochondrial and nuclear gene sequences,
832 with a new tribal classification of the subfamily. BMC Evol. Biol. 8:199.
- 833 Lee C., Blay S., Mooers A.Ø., Singh A., Oakley T.H. 2006. CoMET: A Mesquite package for
834 comparing models of continuous character evolution on phylogenies. Evol.
835 Bioinformatics Online 2:193–196.
- 836 Lu T., Zhu M., Yi C., Si C., Yang C., Chen H. 2017. Complete mitochondrial genome of the
837 gray red-backed vole (*Myodes rufocanus*) and a complete estimate of the phylogenetic
838 relationships in Cricetidae. Mitochondrial DNA Part A 28:62–64.
- 839 Maddin H.C., Jenkins F.A. Jr., Anderson J.S. 2012. The braincase of *Eocaecilia micropodia*
840 (Lissamphibia, Gymnophiona) and the origin of caecilians. PLOS ONE 7:e50743.
- 841 Maddison W.P. 1991. Squared-change parsimony reconstructions of ancestral states for
842 continuous-valued characters on a phylogenetic tree. Syst. Zool. 40:304–314.
- 843 Maddison W.P., Maddison D.R. 2018. Mesquite: a modular system for evolutionary analysis.
844 Version 3.6. <http://mesquite.wikispaces.com>
- 845 Mann A., Pardo J.D., Maddin H.C. 2019. *Infernovenator steenae*, a new serpentine
846 recumbirostran from the ‘Mazon Creek’ *Lagertätte* [sic] further clarifies lysorophian
847 origins. Zool. J. Linn. Soc. online early (12 pp.).
- 848 Marjanović D., Laurin M. 2007. Fossils, molecules, divergence times, and the origin of
849 lissamphibians. Syst. Biol. 56:369–388.
- 850 Marjanović D., Laurin M. 2008. Assessing confidence intervals for stratigraphic ranges of
851 higher taxa: The case of Lissamphibia. Acta Palaeont. Pol. 53:413–432.
- 852 Marjanović D., Laurin M. 2009. The origin(s) of modern amphibians: a commentary. Evol.
853 Biol. 36:336–338.
- 854 Marjanović D., Laurin M. 2013. The origin(s) of extant amphibians: a review with emphasis
855 on the “lepospondyl hypothesis”. Geodiversitas 35:207–272.

- 856 Marjanović D., Laurin M. 2014. An updated paleontological timetree of lissamphibians, with
857 comments on the anatomy of Jurassic crown-group salamanders (Urodela). *Hist. Biol.*
858 26:535–550.
- 859 Marjanović D., Laurin M. 2019. Phylogeny of Paleozoic limbed vertebrates reassessed through
860 revision and expansion of the largest published relevant data matrix. *PeerJ* 6:e5565.
- 861 Maxwell E.E., Harrison L.B., Larsson H.C.E. 2010. Assessing the phylogenetic utility of
862 sequence heterochrony: evolution of avian ossification sequences as a case study.
863 *Zoology* 113:57–66.
- 864 Meredith R.W., Janečka J.E., Gatesy J., Ryder O.A., Fisher C.A., Teeling E.C., Goodbla A.,
865 Eizirik E., Simão T.L.L., Stadler T., Rabosky D.L., Honeycutt R.L., Flynn J.J., Ingram
866 C.M., Steiner C., Williams T.L., Robinson T.J., Burk-Herrick A., Westerman M.,
867 Ayoub N.A., Springer M.S., Murphy W.J. 2011. Impacts of the Cretaceous terrestrial
868 revolution and KPg extinction on mammal diversification. *Science* 334:521–524.
- 869 Milner A.R. 1993. The Paleozoic relatives of lissamphibians. *Herpetol. Monogr.* 7:8–27.
- 870 Olori J.C. 2011. The evolution of skeletal development in early tetrapods: anatomy and
871 ontogeny of microsaur (Lepospondyli) [doctoral thesis]. Austin: University of Texas at
872 Austin. <http://hdl.handle.net/2152/ETD-UT-2011-05-3535>
- 873 Olori J.C. 2013. Ontogenetic sequence reconstruction and sequence polymorphism in extinct
874 taxa: an example using early tetrapods (Tetrapoda: Lepospondyli). *Paleobiology*
875 39:400–428.
- 876 Olori J.C. 2015. Skeletal morphogenesis of *Microbrachis* and *Hyloplesion* (Tetrapoda:
877 Lepospondyli), and implications for the developmental patterns of extinct, early
878 tetrapods. *PLOS ONE* 10:e0128333.
- 879 Pardo J.D., Szostakiwskyj M., Ahlberg P.E., Anderson J.S. 2017a. Hidden morphological
880 diversity among early tetrapods. *Nature* 546:642–645.

- 881 Pardo J.D., Small B.J., Huttenlocker A.K. 2017b. Stem caecilian from the Triassic of
882 Colorado sheds light on the origins of Lissamphibia. *Proc. Natl. Acad. Sci. U.S.A.*
883 114:E5389–E5395.
- 884 Parsons T.S., Williams E.E. 1962. The teeth of Amphibia and their relation to amphibian
885 phylogeny. *J. Morph.* 110:375–389.
- 886 Parsons T.S., Williams E.E. 1963. The relationships of the modern Amphibia: A re-
887 examination. *Q. Rev. Biol.* 38:26–53.
- 888 Pawley K. 2006. The postcranial skeleton of temnospondyls (Tetrapoda: Temnospondyli)
889 [doctoral thesis]. Melbourne: La Trobe University. <http://hdl.handle.net/1959.9/405644>
- 890 Poe S. 2006. Test of von Baer's law of the conservation of early development. *Evolution*
891 60:2239–2245.
- 892 Pons J.-M., Hassanin A., Crochet P.-A. 2005. Phylogenetic relationships within the Laridae
893 (Charadriiformes: Aves) inferred from mitochondrial markers. *Mol. Phyl. Evol.* 37:686–
894 699.
- 895 Prum R.O., Berv J.S., Dornburg A., Field D.J., Townsend J.P., Lemmon A.M., Lemmon A.R.
896 2015. A comprehensive phylogeny of birds (Aves) using targeted next-generation DNA
897 sequencing. *Nature* 526:569–573.
- 898 Pyron R.A. 2014. Biogeographic analysis reveals ancient continental vicariance and recent
899 oceanic dispersal in amphibians. *Syst. Biol.* 63:779–797.
- 900 Rabosky D.L., Donnellan S.C., Grundler M., Lovette I.J. 2014. Analysis and visualization of
901 complex macroevolutionary dynamics: an example from Australian scincid lizards. *Syst.*
902 *Biol.* 63:610–627.
- 903 Reeder T.W. 2003. A phylogeny of the Australian *Sphenomorphus* group (Scincidae:
904 Squamata) and the phylogenetic placement of the crocodile skinks (*Tribolonotus*):
905 Bayesian approaches to assessing congruence and obtaining confidence in maximum

- 906 likelihood inferred relationships. *Mol. Phyl. Evol.* 27:384–397.
- 907 Rineau V., Grand A., Zaragüeta R., Laurin M. 2015. Experimental systematics: sensitivity of
908 cladistic methods to polarization and character ordering schemes. *Contr. Zool.* 84:129–
909 148.
- 910 Rineau V., Zaragüeta i Bagils R., Laurin M. 2018. Impact of errors on cladistic inference:
911 simulation-based comparison between parsimony and three-taxon analysis. *Contr. Zool.*
912 87:25–40.
- 913 Ruta M., Coates M.I. 2007. Dates, nodes and character conflict: addressing the lissamphibian
914 origin problem. *J. Syst. Palaeontol.* 5:69–122.
- 915 Sánchez M. 2012. *Embryos in Deep Time: The Rock Record of Biological Development*. U.
916 of California Press, Berkeley.
- 917 Sánchez-Villagra M.R. 2010. Contributions on fossilised ontogenies: The rock record of
918 vertebrate development. *Semin. Cell Dev. Biol.* 21:399.
- 919 Schneider J.W., Werneburg R., Rößler R., Voigt S., Scholze F. 2015. Example for the
920 description of basins in the CPT Nonmarine-Marine Correlation Chart – Thuringian
921 Forest Basin, East Germany. *Permophiles* 61:29–35.
- 922 Schoch R.R. 2002. The formation of the skull in Paleozoic and extant amphibians.
923 *Paleobiology* 28:378–396.
- 924 Schoch R.R. 2004. Skeleton formation in the Branchiosauridae: a case study in comparing
925 ontogenetic trajectories. *J. Vert. Paleont.* 24:309–319.
- 926 Schoch R.R. 2006. Skull ontogeny: developmental patterns of fishes conserved across major
927 tetrapod clades. *Evol. Dev.* 8:524–536.
- 928 Schoch R.R. 2014a. First evidence of the branchiosaurid temnospondyl *Leptorophus* in the
929 Early Permian of the Saar-Nahe Basin (SW Germany). *N. Jb. Geol. Paläont. Abh.*
930 272:225–236.

- 931 Schoch R.R. 2014b. Amphibian skull evolution: the developmental and functional context of
932 simplification, bone loss and heterotopy. *J. Exp. Zool. (Mol. Dev. Evol.)* 322B:619–630.
- 933 Schoch R.R. 2019. The putative lissamphibian stem-group: phylogeny and evolution of the
934 dissorophoid temnospondyls. *J. Paleont.* 93:37–156.
- 935 Schoch R.R., Carroll R.L. 2003. Ontogenetic evidence for the Paleozoic ancestry of
936 salamanders. *Evol. Dev.* 5:314–324.
- 937 Schoch R.R., Milner A.R. 2004. Structure and implications of theories on the origin of
938 lissamphibians. Pages 345–377 in Arratia G., Wilson M.V.H., Cloutier R., editors.
939 *Recent Advances in the Origin and Early Radiation of Vertebrates*. Munich: Dr.
940 Friedrich Pfeil.
- 941 Sheil C.A., Jorgensen M., Tulenko F., Harrington S. 2014. Variation in timing of ossification
942 affects inferred heterochrony of cranial bones in Lissamphibia. *Evol. Dev.* 16:292–305.
- 943 Sigurdson T., Green D.M. 2011. The origin of modern amphibians: a re-evaluation. *Zool. J.*
944 *Linn. Soc.* 162:457–469.
- 945 Skawiński T., Borczyk B. 2017. Evolution of developmental sequences in lepidosaurs. *PeerJ*
946 5:e3262.
- 947 Spiekman S.N., Werneburg I. 2017. Patterns in the bony skull development of marsupials:
948 high variation in onset of ossification and conserved regions of bone contact. *Sci. Rep.*
949 7:43197.
- 950 Steen M.C. 1938. On the fossil Amphibia from the Gas Coal of Nýřany and other deposits in
951 Czechoslovakia. *Proc. Zool. Soc. Lond.* 108:205–283.
- 952 Sterli J., Pol D., Laurin M. 2013. Incorporating phylogenetic uncertainty on phylogeny-based
953 paleontological dating and the timing of turtle diversification. *Cladistics* 29:233–246.
- 954 Sterli J., de la Fuente M.S., Rougier G.W. 2018. New remains of *Condorchelys antiqua*
955 (Testudinata) from the Early-Middle Jurassic of Patagonia: anatomy, phylogeny, and

- 956 paedomorphosis in the early evolution of turtles. *J. Vert. Paleont.* 38:e1480112.
- 957 Swofford D.L. 2019. PAUP*: Phylogenetic Analysis Using Parsimony (*and other methods),
958 version 4.0a165. Sinauer Associates.
- 959 Tarver J.E., dos Reis M., Mirarab S., Moran R.J., Parker S., O'Reilly J.E., King B.L.,
960 O'Connell M.J., Asher R.J., Warnow T., Peterson K.J., Donoghue P.C.J., Pisani D.
961 2016. The interrelationships of placental mammals and the limits of phylogenetic
962 inference. *Genome Biol. Evol.* 8:330–344.
- 963 van der Vos W., Witzmann F., Fröbisch N.B. 2017. Tail regeneration in the Paleozoic
964 tetrapod *Microbrachis pelikani* and comparison with extant salamanders and squamates.
965 *J. Zool.* 304:34–44.
- 966 Vorobyeva E.I., Hinchliffe J.R. 1996. Developmental pattern and morphology of
967 *Salamendrella keyserlingii* limbs (Amphibia, Hynobiidae) including some
968 evolutionary aspects. *Russ. J. Herpetol.* 1:68–81.
- 969 Wagenmakers E.-J., Farrell S. 2004. AIC model selection using Akaike weights. *Psychon.*
970 *Bull. Rev.* 11:192–196.
- 971 Wang N., Kimball R.T., Braun E.L., Liang B., Zhang Z. 2013. Assessing phylogenetic
972 relationships among Galliformes: a multigene phylogeny with expanded taxon sampling
973 in Phasianidae. *PLOS ONE* 8:1–12.
- 974 Watson D.M.S. 1940. The origin of frogs. *Trans. R. Soc. Edinburgh* 60:195–231.
- 975 Weisbecker V. 2011. Monotreme ossification sequences and the riddle of mammalian skeletal
976 development. *Evolution* 65:1323–1335.
- 977 Weisbecker V., Mitgutsch C. 2010. A large-scale survey of heterochrony in anuran cranial
978 ossification patterns. *J. Zool. Syst. Evol. Research* 48:332–347.
- 979 Werneburg R. 2018 (for 2017). Earliest ‘nursery ground’ of temnospondyl amphibians in the
980 Permian. *Semana* 32:3–42.

- 981 Werneburg I., Geiger M. 2017. Ontogeny of domestic dogs and the developmental
982 foundations of carnivoran domestication. *J. Mammal. Evol.* 24:323–343.
- 983 Werneburg I., Sánchez-Villagra M.R. 2009. Timing of organogenesis support basal position
984 of turtles in the amniote tree of life. *BMC Evol. Biol.* 9:82.
- 985 Witzmann F., Schoch R.R. 2006. Skeletal development of the temnospondyl
986 *Acanthostomatops vorax* from the Lower Permian Döhlen Basin of Saxony. *Trans. R.*
987 *Soc. Edinburgh: Earth Sci.* 96:365–385.
- 988 Zhang P., Zhou H., Chen Y.-Q., Liu Y.-F., Qu L.-H. 2005. Mitogenomic perspectives on the
989 origin and phylogeny of living amphibians. *Syst. Biol.* 54:391–400.
- 990 Zhuang L., Bluteau G., Trueb B. 2015. Phylogenetic analysis of receptor FgfrL1 shows
991 divergence of the C-terminal end in rodents. *Comp. Biochem. Physiol. B* 186:43–50.
- 992
- 993 .

994 FIGURE LEGENDS

995 FIGURE 1. Hypotheses on the relationships of the extant amphibian clades since the late 20th
996 century. The names of terminal taxa sampled here for cranial characters are in boldface, those
997 sampled for appendicular characters are underlined; the names of larger clades are placed
998 toward the right end of a branch if they have minimum-clade (node-based) definitions, to the
999 left if they have maximum-clade (branch-based) definitions. Names in parentheses would,
1000 given that phylogenetic hypothesis, not be used, but replaced by synonyms. Among terminal
1001 taxa, “*Melanerpeton*” *humbergense*, sampled for appendicular characters, is not shown, but is
1002 always the sister-group of *Apateon*; *Microbrachis*, likewise sampled for appendicular
1003 characters, is not shown either, but is always the sister-group of *Hyloplezion*; *Eusthenopteron*
1004 is not shown in c)–h), where it forms the outgroup (b)). For complications involving the
1005 dissorophoid temnospondyl *Micromelerpeton*, see the text. The first two trees (a, b) show the
1006 current consensus; the other trees (c–h) show the various tested paleontological hypotheses.
1007 Abbreviations: D., Dissorophoidea; S., Stereospondylomorpha. a) Consensus of the latest and
1008 largest phylogenetic analyses of molecular data (Irisarri et al. 2017; Feng et al. 2017; Jetz and
1009 Pyron 2018); all named clades are therefore extant. Note the monophyly of the extant
1010 amphibians (Lissamphibia, marked with a light gray dot) with respect to Amniota. b)
1011 Consensus of all analyses of Paleozoic limbed vertebrates (latest and largest: Pawley 2006;
1012 Sigurdsen and Green 2011; Pardo et al. 2017a, b: fig. S6; Marjanović and Laurin 2019; Clack
1013 et al. 2019), omitting the extant amphibian clades. Note the monophyly of “lepospondyls” +
1014 amniotes (marked with a dark gray dot). c) TH: “temnospondyl hypothesis” (most recently
1015 found by Sigurdsen and Green 2011; Maddin et al. 2012; Pardo et al. 2017a, b: fig. S6; argued
1016 for by Schoch and Milner 2004, Schoch 2014b and others). Lissamphibia nested among
1017 dissorophoid temnospondyls. Compatible with both a) and b) (gray dots). d) LH:
1018 “lepospondyl hypothesis” (found most recently by Pawley 2006; Marjanović and Laurin

1019 2009, 2018). Lissamphibia nested among “lepospondyls”; consequently, temnospondyls are
1020 not crown-group tetrapods. Compatible with both a) and b) (gray dots). e) PH1: “polyphyly
1021 hypothesis”, first variant (argued for by Carroll 2001, 2007; Schoch and Carroll 2003; very
1022 cautiously Fröbisch et al. 2007). Urodela as dissorophoid temnospondyls close to *Apateon*,
1023 Anura as a separate clade of dissorophoid temnospondyls, Gymnophiona as “lepospondyls”.
1024 Compatible with b) (dark gray dot) but not with a) (light gray circle). f) PH2: “polyphyly
1025 hypothesis”, second variant (argued for, as one of two options, by Milner 1993). Like PH1,
1026 but with restored monophyly of extant amphibians with respect to amniotes (light gray dot;
1027 see a)) at the expense of compatibility with the paleontological consensus concerning the
1028 position of temnospondyls, lepospondyls, and amniotes (dark gray circle; see b)). g) DH1:
1029 “diphyly hypothesis”, first variant (found by Anderson 2007; Anderson et al. 2008). Batrachia
1030 as dissorophoid temnospondyls, Gymnophiona as “lepospondyls”. Compatible with b) (dark
1031 gray dot) but not with a) (light gray circle). h) DH2: “diphyly hypothesis”, second variant
1032 (found by Pardo et al. 2017b in an analysis that included only temnospondyls and
1033 lissamphibians: fig. 2, S7). Batrachia as dissorophoid temnospondyls, Gymnophiona as
1034 stereospondylomorph temnospondyls . Compatible with both a) and b).

1035 FIGURE 2. Reference phylogeny used for some of the analyses, illustrating the LH
1036 (lepospondyl hypothesis) of lissamphibian origins. The tree was time-calibrated, but analyses
1037 showed that branch lengths are irrelevant, given that the best model is speciation (Tables 2–
1038 4).

1039 FIGURE 3. Strict consensus of the most parsimonious trees obtained by analyzing cranial
1040 dataset 2, which is comprised of 105 taxa and seven characters (see Table 1). Note that
1041 several higher taxa whose monophyly is well-established appear to be para- or polyphyletic
1042 here, which strongly suggests that these data are insufficient to reliably estimate a phylogeny,
1043 but there is clearly a phylogenetic signal because the taxa are not randomly scattered over the

1044 tree. The majority-rule consensus (not shown, but available in SM 1) is more resolved but not
1045 necessarily better because much of the additional resolution contradicts the established
1046 consensus.

1047 FIGURE 4. Strict consensus of the most parsimonious trees obtained by analyzing appendicular
1048 dataset 3, which is comprised of 62 taxa and seven characters (see Table 1). The phylogenetic
1049 signal in these data seems to be lower than in the cranial data. As for the cranial data, the
1050 majority-rule consensus (not shown, but available in SM 1) is more resolved but not
1051 necessarily better because much of the additional resolution contradicts the established
1052 consensus.

1053

1054

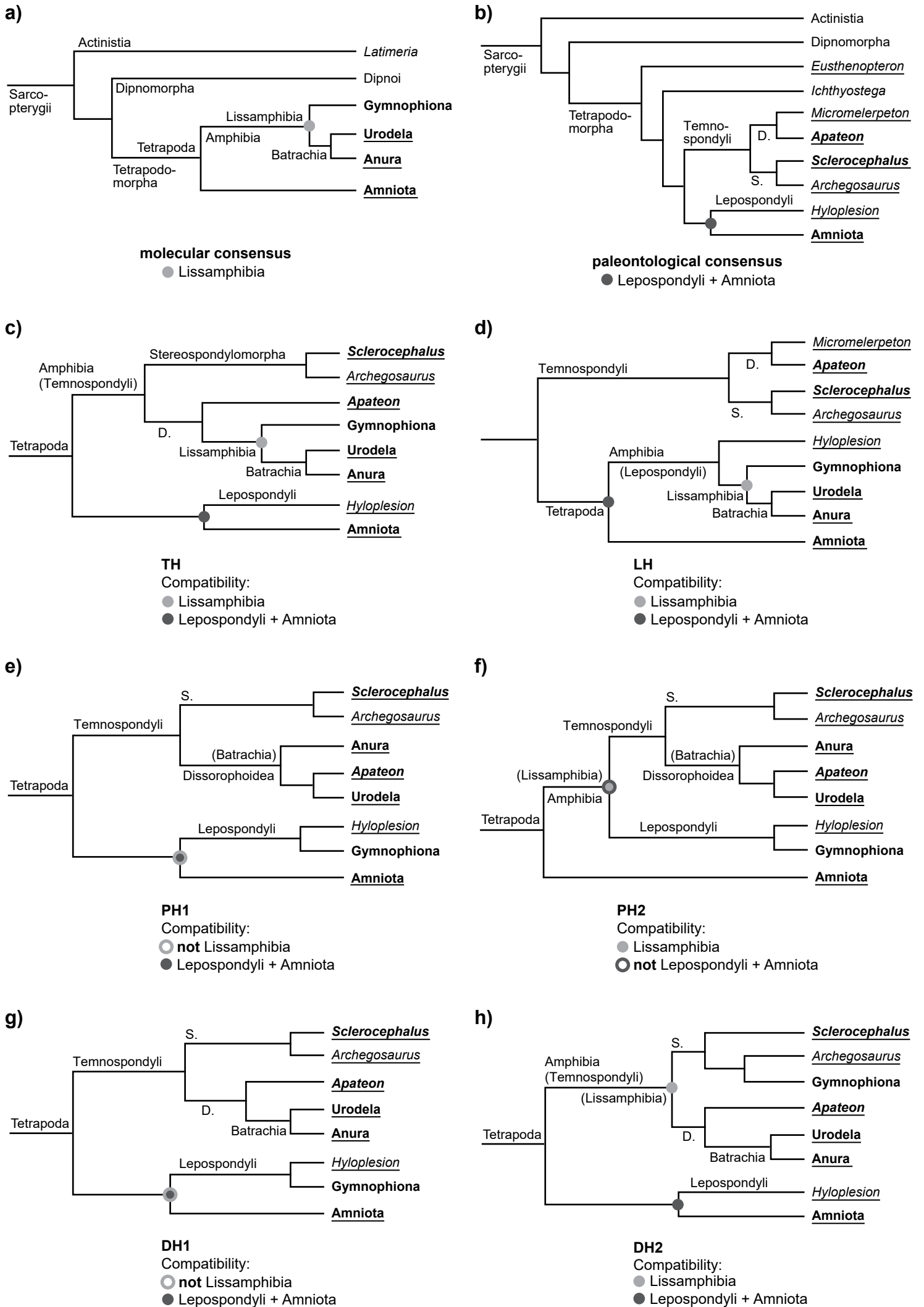


Figure 1

Tree: Cranial analysis from new main tree + Sclerocephalus 6 bones, LH (trees 21-26 were reproduced from this) [21]

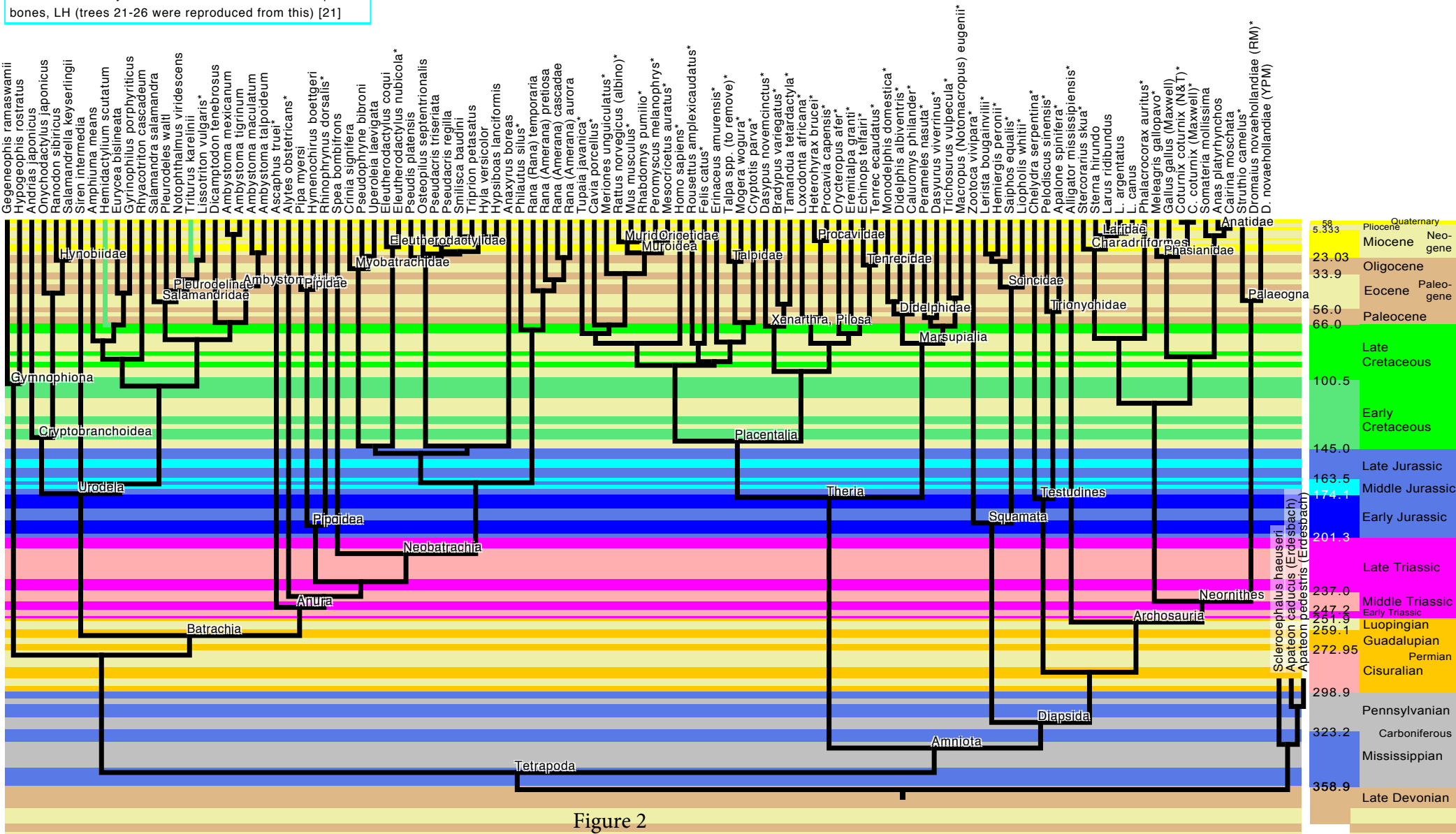


Figure 2

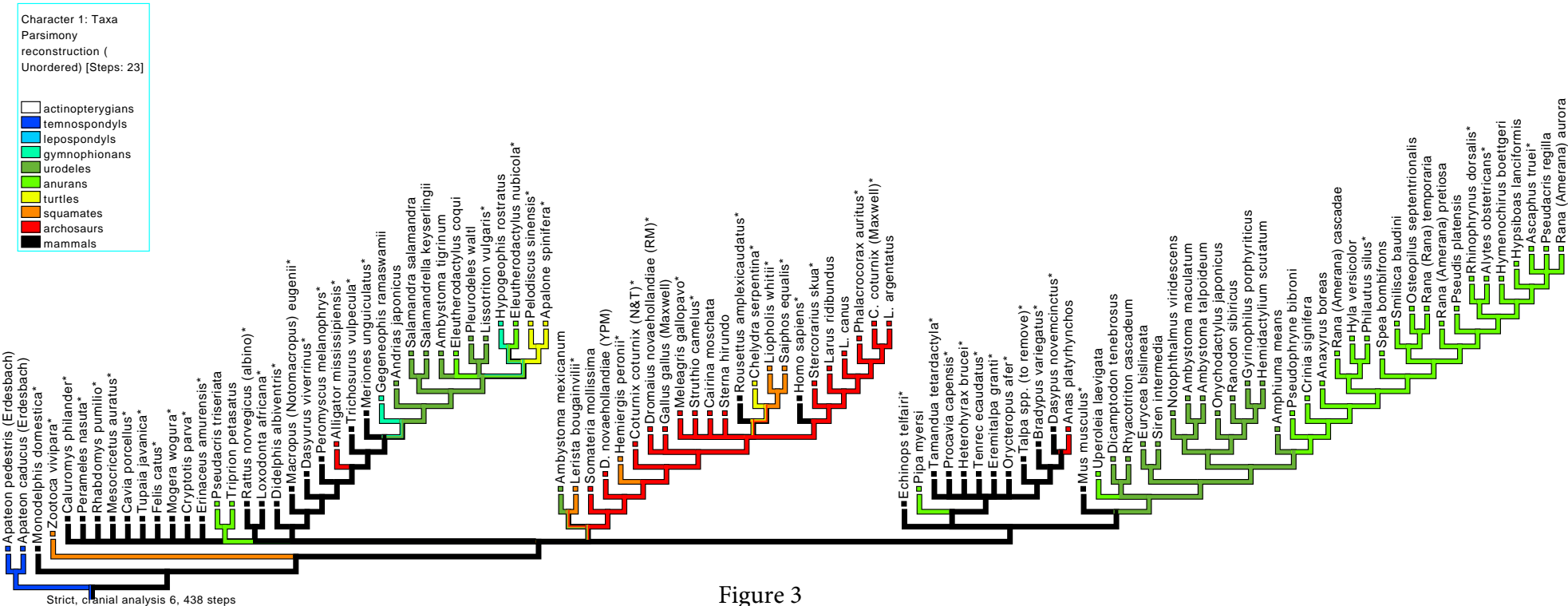


Figure 3

Character 1: Taxa
 Parsimony
 reconstruction (Unordered) [Steps: 28]

- actinopterygians
- temnospondyls
- lepospondyls
- gymnophionans
- urodeles
- anurans
- turtles
- squamates
- archosaurs
- mammals

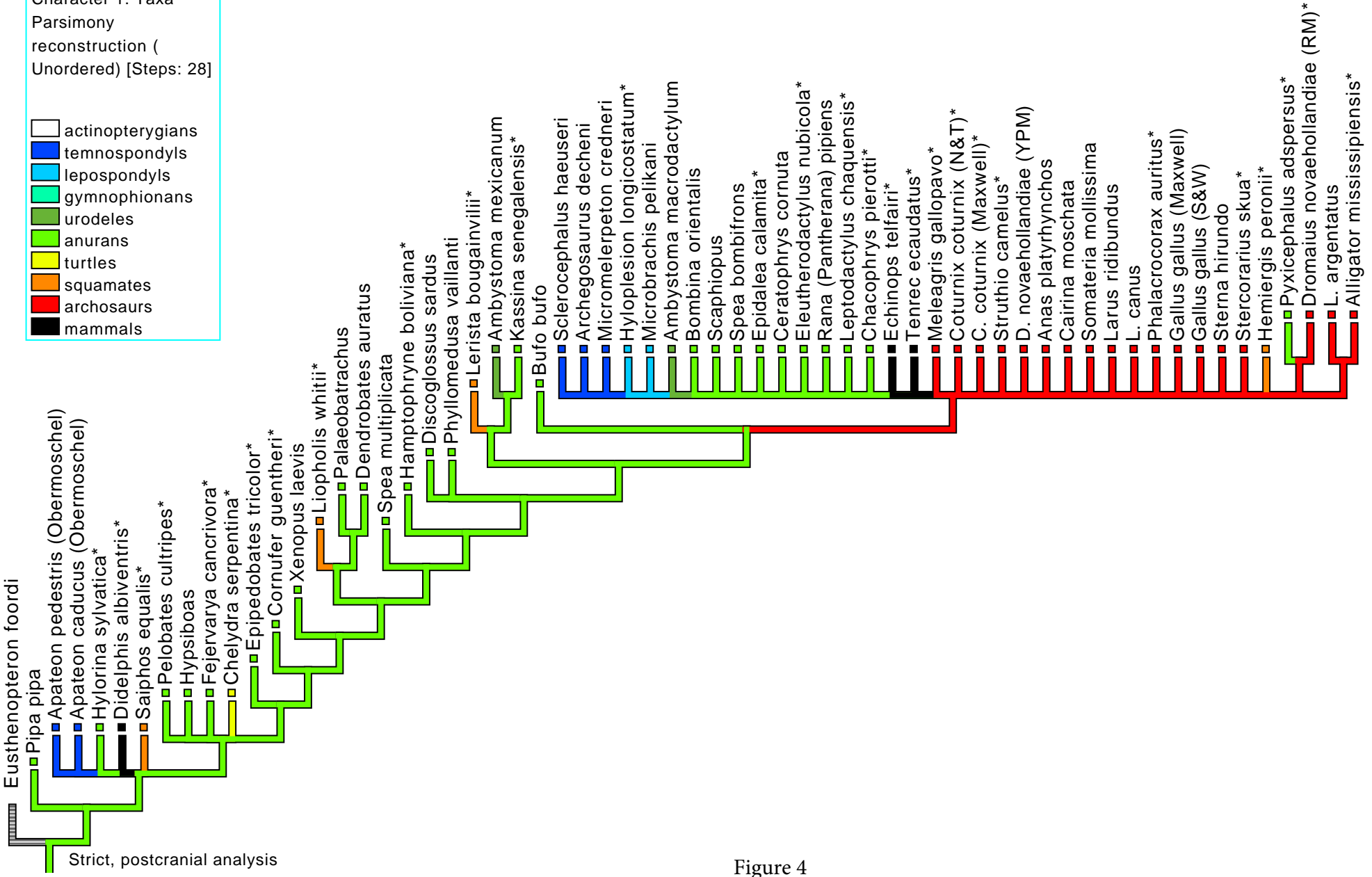


Figure 4

1055 TABLE 1. List of datasets used in this paper. All are subsets of our global compilation that
 1056 were selected to meet the requirement of the method used (missing data cannot be handled).
 1057 The temnospondyl species *Apateon caducus* and *A. pedestris* are included in all datasets, but
 1058 scored after populations from two different paleo-lakes in which both species occur.

Dataset number	1	2	3	4	5
Type of characters	cranial	cranial	appendicular	appendicular	cranial
Number of characters	6	7	7	4	8
Number of taxa	107	105	62	65	84
<i>Sclerocephalus</i>	yes	no	yes	yes	yes
Source of data for <i>Apateon</i>	Erdesbach	Erdesbach	Obermoschel	Erdesbach and Obermoschel	Erdesbach
Additional Paleozoic taxa	None	None	<i>Archegosaurus</i> , <i>Micromelerpeton</i> , <i>Hyloplesion</i> , <i>Microbrachis</i> , <i>Eusthenopteron</i>	<i>Archegosaurus</i> , <i>Micromelerpeton</i> , “ <i>Melanerpeton</i> ” <i>humbergense</i> , <i>Hyloplesion</i> , <i>Microbrachis</i> , <i>Eusthenopteron</i>	None
Table in which it is used	2, 5	3, 6	4, 8	4, 9	7

1059

1060

1061 TABLE 2. Support (AICc and AICc weights) for six evolutionary models given our reference
 1062 tree (LH) and dataset 1 (see Table 1), which comprises six cranial characters (nasal, parietal,
 1063 squamosal, maxilla, pterygoid, and exoccipital) scored in 107 taxa, including the
 1064 temnospondyl *Sclerocephalus*. This was performed on the tree representing the LH
 1065 (lepospondyl hypothesis), but doing this on other trees leads to similar results. Numbers
 1066 presented with four significant digits; best values in boldface. “Distance” refers to keeping the
 1067 original branch lengths (which represent evolutionary time), “equal” sets all branch lengths
 1068 (internal and terminal) to 1, “free” infers them from the data. Abbreviations: k, number of
 1069 estimable parameters; l, likelihood; wi, weight; Δ_i , difference of AICc from that of the Pure-
 1070 Phylogenetic / Equal model.

	AIC	l	k	AICc	Δ_i AICc	wi(AICc)
Pure- Phylogenetic / Distance	-584.4	293.2	1	-583.4	641.2	5.85 E-140
Pure- Phylogenetic / Equal (speciational)	-1225.6	613.8	1	-1224.6	0	1.000
Pure- Phylogenetic / Free	2.000 E10	-1.000 E10	486	2.000 E10	2.000 E10	< E-165
Non- Phylogenetic / Distance	-473.6	237.8	1	-472.6	752.0	4.97 E-164
Non- Phylogenetic / Equal	-959.9	481.0	1	-958.9	265.7	2.02 E-58
Non- Phylogenetic / Free	2.000 E10	-1.000 E10	244	2.000 E10	2.000 E10	< E-165

1071

1072 TABLE 3. Support (AICc and AICc weights) for six evolutionary models given our reference
 1073 tree (LH) and dataset 2 (see Table 1), which comprises seven cranial characters (nasal,
 1074 parietal, squamosal, premaxilla, maxilla, pterygoid, and exoccipital) and 105 taxa, excluding
 1075 *Sclerocephalus*. Abbreviations and boldface as in Table 2.

Evolutionary model	AIC	L	k	AICc	Δ_i AICc	wi(AICc)
Pure-Phylogenetic / Distance	-715.9	359.0	1	-714.9	683.5	< E-26
Pure-Phylogenetic / Equal	-1399.5	700.7	1	-1398.5	0	1.000
Pure-Phylogenetic / Free	2.000 E10	-1.000 E10	306	2.000 E10	2.000 E10	0
Non-Phylogenetic / Distance	-580.6	291.3	1	-579.6	818.8	< E-26
Non-Phylogenetic / Equal	-1106.0	554.0	1	-1105.0	293.5	2.278 E-98
Non-Phylogenetic / Free	2.000 E10	-1.000 E10	244	2.000 E10	2.000 E10	< E-26

1076

1077 TABLE 4. AICc weights showing relative support for six evolutionary models given various
 1078 appendicular datasets (3 and 4; see Table 1) and various hypotheses. Because of the number
 1079 of analyses presented below, only the AICc weights are presented (best values in boldface).
 1080 Abbreviations: DH, diphyly hypothesis (both versions); LH, lepospondyl hypothesis; TH,
 1081 temnospondyl hypothesis.

Evolutionary model	7 characters, LH	7 characters, LH	4 characters, LH	4 characters, TH/DH
Pure-Phylogenetic /				
Distance	5.1857 E-149	2.340 E-70	1.227 E-52	2.646 E-52
Pure-Phylogenetic / Equal	1	0.9335	0.94459	0.8139
Pure-Phylogenetic / Free	< E-179	1.598 E-277	4.012 E-158	3.002 E-155
Non-Phylogenetic /				
Distance	7.515 E-179	4.843 E-52	2.162 E-42	7.262 E-42
Non-Phylogenetic / Equal	2.14914 E-64	6.648 E-02	5.541 E-02	0.1861
Non-Phylogenetic / Free	< E-179	< E-179	< E-179	< E-179

1082

1083

1084 TABLE 5. Support (AIC and AICc weights) for the six topologies, reflecting the six
 1085 hypotheses about the origin of extant amphibians, under the speciation model (called Pure-
 1086 Phylogenetic / Equal in Tables 2–4), with dataset 1 (see Table 1), which includes six cranial
 1087 characters (nasal, parietal, squamosal, maxilla, pterygoid, and exoccipital) and 107 taxa
 1088 (including, among Paleozoic taxa, *Apateon* and *Sclerocephalus*). Abbreviations and boldface
 1089 as in Table 2, except Δ_i : difference of AICc from that of the LH. Hypotheses from top to
 1090 bottom: LH: monophyletic origin from lepospondyls; TH: monophyletic origin among
 1091 temnospondyls; DH1: diphyletic origin, caecilians from lepospondyls and batrachians from
 1092 temnospondyls, as in Anderson et al. (2008); DH2: diphyletic origin (batrachians and
 1093 caecilians from different temnospondyls: Pardo et al. 2017b); PH1: triphyletic (polyphyletic)
 1094 origin with anurans and urodeles from different temnospondyls, caecilians from lepospondyls,
 1095 and lepospondyls closer to Amniota than to Batrachia (Fröbisch et al. 2007); PH2: triphyletic
 1096 (polyphyletic) origin as above, but with lepospondyls and caecilians closer to temnospondyls
 1097 than to amniotes (Milner 1993), reflecting the well-established lissamphibian monophyly
 1098 among extant taxa (e.g. Irisarri et al. 2017; Feng et al. 2017).

Hypothesis	AIC	L	AICc	Δ_i AICc	wi(AICc)
TH	-1217	609.4	-1215	8.919	0.01144
LH	-1226	613.8	-1224	0	0.9885
DH1	-1204	602.9	-1202	21.90	1.738 E-05
DH2	-1195	598.3	-1193	31.01	1.827 E-07
PH1	-1194	597.9	-1192	31.86	1.196 E-07
PH2	-1193	597.4	-1191	32.89	7.143 E-08

1099

1100

1101 TABLE 6. Support (AIC and AICc weights) for the six topologies, reflecting the six
1102 hypotheses about the origin of extant amphibians, for dataset 2 (see Table 1), which includes
1103 seven cranial characters (nasal, parietal, squamosal, premaxilla, maxilla, pterygoid, and
1104 exoccipital) and 105 taxa, excluding *Sclerocephalus* (among Paleozoic taxa, only *Apateon* is
1105 present). Abbreviations, boldface and hypotheses as in Tables 2 and 5.

Hypothesis	AIC	L	AICc	Δ_i AICc	wi(AICc)
TH	-1395	698.6	-1394	4.251	0.1056
LH	-1399	700.7	-1398	0	0.8848
DH1	-1384	693.1	-1383	15.203	4.42 E-4
DH2	-1385	693.6	-1384	14.315	6.89 E-4
PH1	-1387	694.5	-1386	12.404	1.792 E-3
PH2	-1390	695.8	-1388	9.792	6.615 E-3

1106

1107

1108 TABLE 7. Support for the various hypotheses about amphibian origins for dataset 5 (see Table
1109 1), which includes eight cranial characters (frontal added) and 84 taxa, with *Apateon*
1110 sequences from Erdesbach (in addition to *Sclerocephalus* among Paleozoic taxa).
1111 Abbreviations, boldface and hypotheses as in Tables 2 and 5. Because of the taxon sample,
1112 only three topologies can be tested.

Hypothesis	AIC	L	AICc	Δ_i AICc	wi(AICc)
LH	-1296	649.0	-1294	0	0.9935
TH, DH1, DH2	-1286	644.0	-1284	10.061	6.493 E-3
PH	-1274	638.0	-1272	22.038	1.628 E-5

1113

1114

1115 TABLE 8. Support (AICc weights) for the various hypotheses about amphibian origins
 1116 according to dataset 3 (see Table 1), which features seven appendicular characters (humerus,
 1117 radius, ulna, ilium, femur, tibia and fibula) and 62 taxa, including several Paleozoic taxa (the
 1118 temnospondyls *Archegosaurus decheni* and *Micromelerpeton credneri*, the lepospondyls
 1119 *HylopleSION longicaudatum* and *Microbrachis pelikani*, and the tristichopterid *Eusthenopteron*
 1120 *foordi*) in addition to *Apateon* (two species, *A. caducus* and *A. pedestris*) and *Sclerocephalus*
 1121 *haeuseri*. The *Apateon* sequences come from Obermoschel. Abbreviations, boldface and
 1122 hypotheses as in Table 5, except that the TH and both variants of the DH become
 1123 indistinguishable, but the phylogenetic position of the “branchiosaur” *Micromelerpeton* can
 1124 be tested.

Hypothesis	AIC	l	AICc	Δ_i AICc	wi(AICc)
LH	-885.0	443.5	-884.2	11.808	2.177 E-3
TH, DH (branchiosaur monophyly)	-881.1	441.6	-880.3	2.897	0.1874
TH, DH (branchiosaur polyphyly)	-886.4	444.2	-885.6	15.754	3.027 E-4
PH1	-888.5	445.3	-887.7	8.341	0.01232
PH2	-896.9	449.4	-896.1	0.000	0.7978

1125

1126

1127 TABLE 9. Effect of the intraspecific variability in ossification sequences of *Apateon* on the
 1128 support (AICc weight; best values in boldface) for the various hypotheses about amphibian
 1129 origins. The dataset (number 4; Table 1) includes only four appendicular bones (radius, ulna,
 1130 ilium, and femur) and 63 to 65 taxa but it allows testing the impact of infraspecific variability
 1131 in ossification sequences in *Apateon*, which are documented in two localities (Erdesbach and
 1132 Obermoschel). Because of the number of tests presented (15: five topologies x three sets of
 1133 sequences), only the AICc weights are given. In all tests, the following Paleozoic taxa are
 1134 present: *Sclerocephalus haeuseri*, *Archegosaurus decheni*, “*Melanerpeton*” *humbergense*,
 1135 *Micromelerpeton credneri*, *Apateon* (two species, *A. caducus* and *A. pedestris*) among
 1136 temnospondyls, *Hyloplecion longicaudatum* and *Microbrachis pelikani* among lepospondyls,
 1137 and the tristichopterid *Eusthenopteron foordi*. For abbreviations of the hypotheses, see Table
 1138 5.

Hypothesis	Erdesbach and Obermoschel	Erdesbach	Obermoschel
LH	0.21407	0.20169	0.22657
TH, DH (branchiosaur monophyly)	0.05492	0.05265	0.05532
TH, DH (branchiosaur polyphyly)	0.03713	0.04285	0.03342
PH1	0.05653	0.05491	0.05638
PH2	0.63735	0.64790	0.62832

1139

1140 **Appendix 1: Sources of data for ossification sequences.**

1141

1142 Empty cells indicate that these data are unavailable. Three methods were examined, and we
1143 used the one for which most data were available (position in the ossification sequence, last
1144 column).

Standardization method (data type used)

Taxa	Ontogenetic stages	Snout-vent length (mm)	Ossification sequence position
------	--------------------	------------------------	--------------------------------

Actinopterygii

<i>Amia calva</i>		Grande and Bemis 1998	Grande and Bemis 1998
<i>Clarias gariepinus</i>		Adriaens and Verraes 1998	Adriaens and Verraes 1998
<i>Danio rerio</i>		Cubbage and Mabee 1996	Cubbage and Mabee 1996
<i>Oryzias latipes</i>	Langille and Hall 1987		

Tristichopteridae

<i>Eusthenopteron foordi</i>		Cote et al. 2002; Leblanc and Cloutier 2005	Cote et al. 2002; Leblanc and Cloutier 2005
------------------------------	--	--	--

Temnospondyli

<i>Archegosaurus decheni</i>		Witzmann 2006	Witzmann 2006
------------------------------	--	---------------	---------------

<i>Apateon caducus</i> (Erdesbach)	Schoch 2004	Schoch 2004	Schoch 2004
<i>Apateon caducus</i> (Obermoschel)		Werneburg 2018	Werneburg 2018
<i>Apateon pedestris</i> (Erdesbach)	Schoch 2004		Schoch 2004
<i>Apateon pedestris</i> (Obermoschel)		Werneburg 2018	Werneburg 2018
“ <i>Melanerpeton</i> ” <i>humbergense</i>	Schoch 2004		Schoch 2004
<i>Micromelerpeton credneri</i>		Boy 1995; Lillich and Schoch 2007; Witzmann and Pfretzschner 2009; Schoch 2009	Boy 1995; Lillich and Schoch 2007; Witzmann and Pfretzschner 2009; Schoch 2009
<i>Sclerocephalus haeuseri</i>	Lohmann and Sachs 2001; Schoch 2003; Schoch and Witzmann 2009; Werneburg 2018	Lohmann and Sachs 2001; Schoch 2003; Schoch and Witzmann 2009; Werneburg 2018	Lohmann and Sachs 2001; Schoch 2003; Schoch and Witzmann 2009; Werneburg 2018
Lepospondyli			
<i>Hyloplesion longicaudatum</i>		Olori 2013	Olori 2013
<i>Microbrachis pelikani</i>		Olori 2013	Olori 2013

Gymnophiona

Gegeneophis ramaswamii Müller et al. 2005 Harrington et al. 2013

Hypogeophis rostratus Müller 2006 Harrington et al. 2013

Urodela

Aneides lugubris Wake et al. 1983 Wake et al. 1983

Ambystoma macrodactylum Harrington et al. 2013

Ambystoma maculatum Moore 1989 Harrington et al. 2013

Ambystoma mexicanum Laurin and
Germain 2011 Harrington et al. 2013

Ambystoma talpoideum Reilly 1987 Reilly 1987 Reilly 1987

Ambystoma texanum Laurin and
Germain 2011 Harrington et al. 2013

Ambystoma tigrinum Harrington et al. 2013

Amphiuma means Harrington et al. 2013

Andrias japonicus Harrington et al. 2013

Bolitoglossa subpalmata Ehmcke and Clemen
2000

Dicamptodon tenebrosus Harrington et al. 2013

Eurycea bislineata Harrington et al. 2013

Gyrinophilus porphyriticus Harrington et al. 2013

Hemidactylium scutatum Harrington et al. 2013

Lissotriton vulgaris Laurin and
Germain 2011 Harrington et al. 2013

<i>Necturus maculosus</i>			Harrington et al. 2013
<i>Notophthalmus viridescens</i>	Reilly 1986	Reilly 1986	Harrington et al. 2013
<i>Onychodactylus japonicus</i>			Harrington et al. 2013
<i>Pleurodeles waltl</i>			Harrington et al. 2013
<i>Ranodon sibiricus</i>			Harrington et al. 2013
<i>Salamandra salamandra</i>			Harrington et al. 2013
<i>Salamandrella keyserlingii</i>			Harrington et al. 2013
<i>Siren intermedia</i>	Reilly and Altig 1996	Reilly and Altig 1996	Reilly and Altig 1996
<i>Triturus karelinii</i>			Harrington et al. 2013
Anura			
<i>Alytes obstetricans</i>			Yeh 2002
<i>Ascaphus truei</i>			Harrington et al. 2013
<i>Anaxyrus boreas</i>			Gaudin 1978
<i>Bombina orientalis</i>			Harrington et al. 2013
<i>Bufo bufo</i>			Harrington et al. 2013
<i>Cornufer guentheri</i>			Harrington et al. 2013
<i>Ceratophrys cornuta</i>			Harrington et al. 2013
<i>Chacophrys pierotti</i>			Harrington et al. 2013
<i>Crinia signifera</i>			Harrington et al. 2013
<i>Dendrobates auratus</i>	de Sá and Hill 1998	de Sá and Hill 1998	Harrington et al. 2013
<i>Discoglossus sardus</i>			Pugener and Maglia 1997
<i>Eleutherodactylus coqui</i>			Harrington et al. 2013

<i>Eleutherodactylus nubicola</i>			Harrington et al. 2013
<i>Epidalea calamita</i>			Harrington et al. 2013
<i>Epipedobates tricolor</i>	de Sá and Hill 1998	de Sá and Hill 1998	Harrington et al. 2013
<i>Fejervarya cancrivora</i>			Harrington et al. 2013
<i>Hamptophryne boliviana</i>			Harrington et al. 2013
<i>Hyla versicolor</i>			Harrington et al. 2013
<i>Hylorina sylvatica</i>			Harrington et al. 2013
<i>Hymenochirus boettgeri</i>			de Sá and Swart 1999
<i>Hypsiboas lanciformis</i>	de Sá 1988	de Sá 1988	de Sá 1988
<i>Kassina senegalensis</i>			Harrington et al. 2013
<i>Leptodactylus chaquensis</i>			Harrington et al. 2013
<i>Osteopilus septentrionalis</i>			Trueb 1966
<i>Palaeobatrachus sp.</i>			Harrington et al. 2013
<i>Pelobates cultripes</i>			Harrington et al. 2013
<i>Philautus silus</i>			Harrington et al. 2013
<i>Phyllomedusa vaillanti</i>			Harrington et al. 2013
<i>Pipa myersi</i>			Yeh 2002
<i>Pipa pipa</i>		Trueb et al. 2000	Harrington et al. 2013
<i>Pseudacris regilla</i>			Harrington et al. 2013
<i>Pseudacris triseriata</i>			Harrington et al. 2013
<i>Pseudis platensis</i>			Harrington et al. 2013
<i>Pseudophryne bibronii</i>			Harrington et al. 2013
<i>Pyxicephalus adspersus</i>			Harrington et al. 2013
<i>Rana (Amerana) aurora</i>			Harrington et al. 2013

<i>Rana (Amerana) cascadae</i>			Harrington et al. 2013
<i>Rana (Amerana) pretiosa</i>			Harrington et al. 2013
<i>Rana (Rana) temporaria</i>			Harrington et al. 2013
<i>Rana (Pantherana) pipiens</i>			Kemp and Hoyt 1969
<i>Rhinophrynus dorsalis</i>			Harrington et al. 2013
<i>Shomronella jordánica</i>			Harrington et al. 2013
<i>Smilisca baudini</i>			Harrington et al. 2013
<i>Spea bombifrons</i>	Wiens 1989	Wiens 1989	Wiens 1989
<i>Spea multiplicata</i>			Harrington et al. 2013
<i>Tripurion petasatus</i>			Harrington et al. 2013
<i>Uperoleia laevigata</i>			Harrington et al. 2013
<i>Xenopus laevis</i>			Harrington et al. 2013
Mammalia			
<i>Bradypus variegatus</i>			Hautier et al. 2011
<i>Cavia porcellus</i>			Hautier et al. 2013
<i>Choloepus didactylus</i>			Hautier et al. 2011
<i>Cryptotis parva</i>			Koyabu et al. 2011
<i>Cyclopes didactylus</i>			Hautier et al. 2011
<i>Dasypus novemcinctus</i>			Hautier et al. 2011
<i>Dasyurus viverrinus</i>			Hautier et al. 2013
<i>Didelphis albiventris</i>		de Oliveira et al. 1998	de Oliveira et al. 1998
<i>Echinops telfairi</i>			Werneburg et al. 2013
<i>Elephantulus rozeti</i>			Hautier et al. 2013
<i>Eremitalpa granti</i>			Hautier et al. 2013

<i>Erinaceus amurensis</i>		Koyabu et al. 2011
<i>Felis silvestris</i>		Sánchez-Villagra et al. 2008
<i>Homo sapiens</i>		Hautier et al. 2013
<i>Heterohyrax brucei</i>		Hautier et al. 2013
<i>Loxodonta africana</i>		Hautier et al. 2012
<i>Macropus eugenii</i>		Hautier et al. 2013
<i>Macroscelides proboscideus</i>		Hautier et al. 2013
<i>Manis javanica</i>		Hautier et al. 2013
<i>Meriones unguiculatus</i>	Yukawa et al. 1999	Yukawa et al. 1999
<i>Mesocricetus auratus</i>		Hautier et al. 2013
<i>Mogera wogura</i>		Koyabu et al. 2011
<i>Monodelphis domestica</i>		Hautier et al. 2013
<i>Mus musculus</i>		Hautier et al. 2013
<i>Ornithorhynchus anatinus</i>		Weisbecker 2011
<i>Orycteropus afer</i>		Hautier et al. 2013
<i>Perameles nasuta</i>		Hautier et al. 2013
<i>Peromyscus melanophrys</i>		Hautier et al. 2013
<i>Procavia capensis</i>		Hautier et al. 2013
<i>Rattus norvegicus</i>		Hautier et al. 2013
<i>Rhabdomys pumilio</i>		Hautier et al. 2013
<i>Rousettus amplexicaudatus</i>		Hautier et al. 2013
<i>Sus scrofa</i>		Hautier et al. 2013
<i>Tachyglossus aculeatus</i>		Weisbecker 2011

<i>Talpa</i> spp.		Sánchez-Villagra et al. 2008
<i>Tenrec ecaudatus</i>		Werneburg et al. 2013
<i>Tamandua tetradactyla</i>		Hautier et al. 2011
<i>Tarsius spectrum</i>		Hautier et al. 2013
<i>Trichosurus vulpecula</i>	Weisbecker et al. 2008	Hautier et al. 2013
<i>Tupaia javanica</i>		Hautier et al. 2013
Squamata		
<i>Lacerta vivipara</i>		Hautier et al. 2013
<i>Lerista bougainvillii</i>	Hugi et al. 2012	Hugi et al. 2012
<i>Liopholis whitii</i>	Hugi et al. 2012	Hugi et al. 2012
<i>Hemiergus peronii</i>	Hugi et al. 2012	Hugi et al. 2012
<i>Saiphos equalis</i>	Hugi et al. 2012	Hugi et al. 2012
Crocodylia		
<i>Alligator mississippiensis</i>	Rieppel 1993a	Rieppel 1993a
Aves		
<i>Anas platyrhynchos</i>		Maxwell et al. 2010
<i>Cairina moschata</i>		Maxwell et al. 2010
<i>Coturnix coturnix</i>		Maxwell et al. 2010
<i>Coturnix coturnix</i> (N&T)		Maxwell et al. 2010
<i>Dromaius novaehollandiae</i>		Maxwell et al. 2010
<i>Dromaius novaehollandiae</i> (YPM)		Maxwell et al. 2010

<i>Gallus gallus</i>			Maxwell et al. 2010
<i>Gallus gallus</i> (S&W)			Maxwell et al. 2010
<i>Larus argentatus</i>			Maxwell et al. 2010
<i>Larus canus</i>			Maxwell et al. 2010
<i>Larus ridibundus</i>			Maxwell et al. 2010
<i>Meleagris gallopavo</i>			Maxwell et al. 2010
<i>Phalacrocorax auritus</i>			Maxwell et al. 2010
<i>Somateria mollissima</i>			Maxwell et al. 2010
<i>Stercorarius skua</i>			Maxwell et al. 2010
<i>Sterna hirundo</i>			Maxwell et al. 2010
<i>Struthio camelus</i>			Maxwell et al. 2010

Testudines

<i>Apalone spinifera</i>			Sánchez-Villagra et al. 2008
<i>Chelydra serpentina</i>	Rieppel 1993b	Rieppel 1990, 1993b	Rieppel 1993b
<i>Macrochelys temminckii</i>			Sánchez-Villagra et al. 2008
<i>Pelodiscus sinensis</i>			Sánchez-Villagra et al. 2008

1145

1146

1147 **Appendix references**

- 1148 Adriaens D., Verraes W. 1998. Ontogeny of the osteocranium in the African Catfish, *Clarias*
1149 *gariiepinus* Burchell (1822) (Siluriformes: Clariidae): ossification sequence as a
1150 response to functional demands. *J. Morph.* 235:183–237.
- 1151 Boy J. 1995. Über die Micromelerpetontidae (Amphibia: Temnospondyli). 1. Morphologie
1152 und Paläoökologie des *Micromelerpeton credneri* (Unter-Perm; SW-Deutschland).
1153 *Paläont. Z.* 69:429–457.
- 1154 Cote S., Carroll R., Cloutier R., Bar-Sagi L. 2002. Vertebral development in the Devonian
1155 sarcopterygian fish *Eusthenopteron foordi* and the polarity of vertebral evolution in non-
1156 amniote tetrapods. *J. Vertebr. Paleontol.* 22:487–502.
- 1157 Cubbage C.C., Mabee P.M. 1996. Development of the cranium of paired fins in the Zebrafish
1158 *Danio rerio* (Ostariophysi, Cyprinidae). *J. Morph.* 229:121–160.
- 1159 Ehmcke J., Clemen G. 2000. The structure and development of the skull of Costa Rican
1160 plethodontid salamanders (Amphibia: Urodela). *Ann. Anat.* 182: 537–547.
- 1161 Gaudin A.J. 1978. The sequence of cranial ossification in the California toad, *Bufo boreas*
1162 (Amphibia, Anura, Bufonidae). *J. Herpetol.* 12:309–318.
- 1163 Grande L., Bemis W.E. 1998. A comprehensive phylogenetic study of amiid fishes (Amiidae)
1164 based on comparative skeletal anatomy. An empirical search for interconnected patterns
1165 of natural history. *J. Vertebr. Paleontol.* 18(1, suppl.; Soc. of Vert. Paleont. Memoir
1166 4):688 pages.
- 1167 Hautier L., Weisbecker V., Goswami A., Knight F., Kardjilov N., Asher R. J. 2011. Skeletal
1168 ossification and sequence heterochrony in xenarthran evolution. *Evol. Dev.* 13:460–476.
- 1169 Hautier L., Stansfield F. J., Allen W. R., Asher R. J. 2012. Skeletal development in the
1170 African elephant and ossification timing in placental mammals. *Proc. R. Soc. B*
1171 279:2188–2195.

- 1172 Hautier L., Bennett N.C., Viljoen H., Howard L., Milinkovitch M.C., Tzika A.C., Goswami
1173 A., Asher R.J. 2013. Patterns of ossification in southern versus northern placental
1174 mammals: mammal skeletogenesis. *Evolution* 67:1994–2010.
- 1175 Harrington S.M., Harrison L.B., Sheil C.A. 2013. Ossification sequence heterochrony among
1176 amphibians. *Evol. Dev.* 15:344–364.
- 1177 Hugi J., Hutchinson M.N., Koyabu D., Sánchez-Villagra M.R. 2012. Heterochronic shifts in
1178 the ossification sequences of surface- and subsurface-dwelling skinks are correlated with
1179 the degree of limb reduction. *Zoology* 115:188–198.
- 1180 Kemp N. E. and Hoyt J. 1969. Sequence of ossification in the skeleton of growing and
1181 metamorphosing tadpoles of *Rana pipiens*. *J. Morphol.* 129:415–444.
- 1182 Koyabu D., Endo H., Mitgutsch C., Suwa G., Catania K. C., Zollikofer C. P. E., Oda S.,
1183 Koyasu K., Ando M., Sánchez-Villagra M. R. 2011. Heterochrony and developmental
1184 modularity of cranial osteogenesis in lipotyphlan mammals. *EvoDevo* 2:1–18.
- 1185 Laurin M., Germain D. 2011. Developmental characters in phylogenetic inference and their
1186 absolute timing information. *Syst. Biol.* 60:630–644.
- 1187 Langille R.M., Hall B.K. 1987. Development of the head skeleton of the Japanese medaka,
1188 *Oryzias latipes* (Teleostei). *J. Morphol.* 193:135–158.
- 1189 Leblanc J., Cloutier R. 2005. Developmental modularity and saltatory ontogeny in the Late
1190 Devonian osteolepiform *Eusthenopteron foordi*. Pp. 32–84 in Leblanc J: Précisions sur
1191 l’anatomie de l’ostéolépiforme *Eusthenopteron foordi* du Dévonien supérieur de
1192 Miguasha, Québec. Mémoire de maîtrise (~ M.Sc. thesis), Université du Québec à
1193 Rimouski. Available at http://semaphore.uqar.ca/283/1/Joel_Leblanc_aout2005.pdf
- 1194 Lillich R., Schoch R. 2007. Finally grown up—the significance of adult *Micromelerpeton*
1195 [abstract]. *J. Vert. Paleontol.* 27(3, suppl.):106A.

- 1196 Lohmann U., Sachs S. 2001. Observations on the postcranial morphology, ontogeny and
1197 palaeobiology of *Sclerocephalus haeuseri* (Amphibia: Actinodontidae) from the Lower
1198 Permian of Southwest Germany. Mem. Queensland Mus. 46:771–781.
- 1199 Maxwell E.E., Harrison L.B., Larsson H.C.E. 2010. Assessing the phylogenetic utility of
1200 sequence heterochrony: evolution of avian ossification sequences as a case study.
1201 Zoology 113:57–66.
- 1202 Müller H., Oommen O.V., Bartsch P. 2005. Skeletal development of the direct-developing
1203 caecilian *Gegeneophis ramaswamii* (Amphibia: Gymnophiona: Caeciliidae).
1204 Zoomorphology 124:171–188.
- 1205 Müller H. 2006. Ontogeny of the skull, lower jaw, and hyobranchial skeleton of *Hypogeophis*
1206 *rostratus* (Amphibia: Gymnophiona: Caeciliidae) revisited. J. Morph. 267:968–986.
- 1207 de Oliveira C.A., Nogueira J.C., Mahecha G.A.B. 1998. Sequential order of appearance of
1208 ossification centers in the opossum *Didelphis albiventris* (Didelphidae) skeleton during
1209 development in the Marsupium. Ann. Anat. 180:113–121. [Lack of italics in the
1210 original.]
- 1211 Olori, J.C. 2013. Ontogenetic sequence reconstruction and sequence polymorphism in extinct
1212 taxa: an example using early tetrapods (Tetrapoda: Lepospondyli). Paleobiology
1213 39:400–428.
- 1214 Púgener L.A., Maglia A.M. 1997. Osteology and skeletal development of *Discoglossus*
1215 *sardus* (Anura: Discoglossidae). J. Morphol. 233:267–286.
- 1216 Reilly S.M. 1986. Ontogeny of cranial ossification in the eastern newt, *Notophthalmus*
1217 *viridescens* (Caudata: Salamandridae), and its relationship to metamorphosis and
1218 neoteny. J. Morphol. 188:315–326.

- 1219 Reilly S.M. 1987. Ontogeny of the hyobranchial apparatus in the salamanders *Ambystoma*
1220 *talpoideum* (Ambystomatidae) and *Notophthalmus viridescens* (Salamandridae): the
1221 ecological morphology of two neotenic strategies. *J. Morphol.* 191:205–214.
- 1222 Reilly S.M., Altig R. 1996. Cranial ontogeny in *Siren intermedia* (Amphibia: Sirenidae):
1223 Paedomorphic, metamorphic, and novel patterns of heterochrony. *Copeia* 1996:29–41.
- 1224 Rieppel O. 1990. The structure and development of the jaw adductor musculature in the turtle
1225 *Chelydra serpentina*. *Zool. J. Linn. Soc.* 98:27–62.
- 1226 Rieppel O. 1993a. Studies on skeleton formation in reptiles. V. Patterns of ossification in the
1227 skeleton of *Alligator mississippiensis* Daudin (Reptilia, Crocodylia). *Zool. J. Linn. Soc.*
1228 109:301–325.
- 1229 Rieppel O. 1993b. Studies on skeleton formation in reptiles: Patterns of ossification in the
1230 skeleton of *Chelydra serpentina* (Reptilia, Testudines). *J. Zool. (Lond.)* 231:487–509.
- 1231 Sánchez-Villagra M., Goswami A., Weisbecker V., Mock O., Kuratani S. 2008. Conserved
1232 relative timing of cranial ossification patterns in early mammalian evolution. *Evol.*
1233 *Dev.* 10:519–530.
- 1234 de Sá R.O. 1988. Chondrocranium and ossification sequence of *Hyla lanciformis*. *J. Morphol.*
1235 195:345–355.
- 1236 de Sá R.O., Swart C.C. 1999. Development of the suprarostrals plate of pipoid frogs. *J.*
1237 *Morphol.* 240:143–153.
- 1238 Schoch R.R. 2004. Skeleton formation in the Branchiosauridae: a case study in comparing
1239 ontogenetic trajectories. *J. Vert. Paleontol.* 24:309–319.
- 1240 Schoch R.R. 2003. Early larval ontogeny of the Permo-Carboniferous temnospondyl
1241 *Sclerocephalus*. *Palaeontology* 46:1055–1072.
- 1242 Schoch R.R. 2009. Evolution of life cycles in early amphibians. *Annu. Rev. Earth Planet. Sci.*
1243 37:125–162.

- 1244 Schoch R.R., Witzmann F. 2009. Osteology and relationships of the temnospondyl genus
1245 *Sclerocephalus*. Zool. J. Linn. Soc. 157:135–168.
- 1246 Trueb L. 1966. Morphology and development of the skull in the frog *Hyla septentrionalis*.
1247 Copeia 1966:562–573.
- 1248 Trueb L., Pugener L.A., Maglia A.M. 2000. Ontogeny of the bizarre: An osteological
1249 description of *Pipa pipa* (Anura: Pipidae), with an account of skeletal development in
1250 the species. J. Morphol. 243:75–104.
- 1251 Wake T.A., Wake D.B., Wake M.H. 1983. The ossification sequence of *Aneides lugubris*,
1252 with comments on heterochrony. J. Herpetol. 17:10–22.
- 1253 Weisbecker V., Goswami A., Wroe S., Sánchez-Villagra M.R. 2008. Ossification
1254 heterochrony in the therian postcranial skeleton and the marsupial–placental dichotomy.
1255 Evolution 62:2027–2041.
- 1256 Weisbecker V. 2011. Monotreme ossification sequences and the riddle of mammalian skeletal
1257 development. Evolution 65:1323–1335.
- 1258 Werneburg R. 2018 (for 2017). Earliest ‘nursery ground’ of temnospondyl amphibians in the
1259 Permian. Semana 32:3–42.
- 1260 Werneburg I., Tzika A.C., Hautier L., Asher R.J., Milinkovitch M.C., Sánchez-Villagra M.R.
1261 2013. Development and embryonic staging in non-model organisms: the case of an
1262 afrotherian mammal: Development and embryonic staging. J. Anat. 222:2–18.
- 1263 Wiens J.J. 1989. Ontogeny of the skeleton of *Spea bombifrons* (Anura: Pelobatidae). J.
1264 Morphol. 202:29–51.
- 1265 Witzmann F. 2006. Developmental patterns and ossification sequence in the Permo-
1266 Carboniferous temnospondyl *Archegosaurus decheni* (Saar-Nahe Basin, Germany). J.
1267 Vert. Paleontol. 26:7–17.

- 1268 Witzmann F., Pfretzschner H.-U. 2003. Larval ontogeny of *Micromelerpeton credneri*
1269 (Temnospondyli, Dissorophoidea). *J. Vert. Paleontol.* 23:750–768.
- 1270 Yeh J. 2002. The evolution of development: two portraits of skull ossification in pipoid frogs.
1271 *Evolution* 56:2484–2498.
- 1272 Yukawa M., Hayashi N., Takagi K., Mochizuki K. 1999. The normal development of
1273 Mongolian Gerbil fetuses and, in particular, the timing and sequence of the appearance
1274 of ossification centres. *Anat. Histol. Embryol.* 28:319–324.
- 1275
- 1276

1277 SUPPLEMENTARY MATERIAL

1278 Data matrix in NEXUS format for Mesquite.

1279